

ASSESSING THE REFLECTANCE SPECTRA OF OBSIDIANS AS A POSSIBLE TOOL FOR AGE DETERMINATION OF HOLOCENE LAVAS

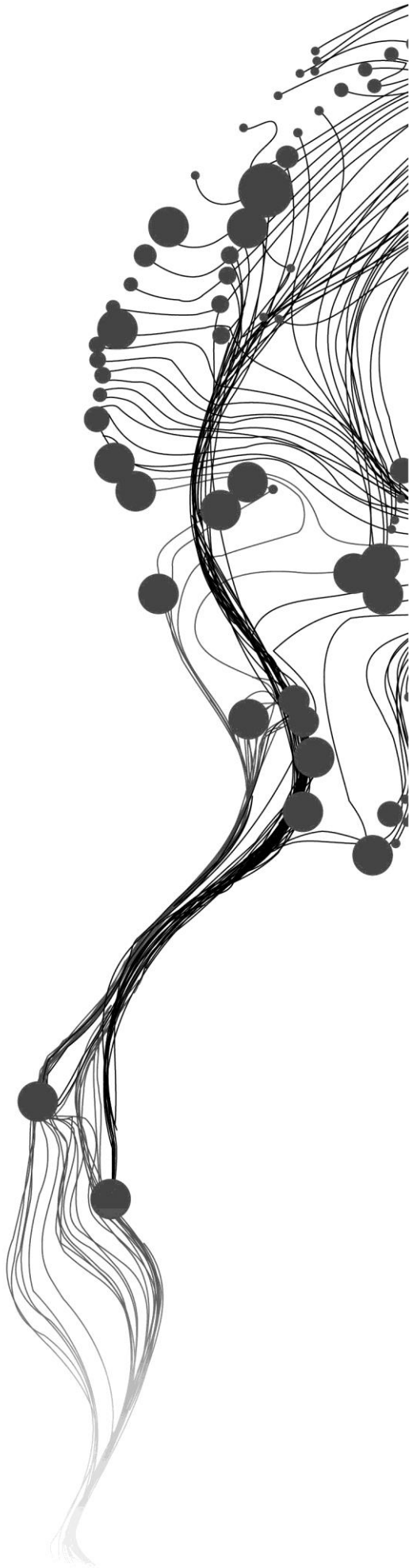
YEWUBINESH BEKELE REBA

February, 2016

SUPERVISORS:

Dr. C.A. (Chris) Hecker

Dr. F.J.A. (Frank) Van Ruitenbeek



ASSESSING THE REFLECTANCE SPECTRA OF OBSIDIANS AS A POSSIBLE TOOL FOR AGE DETERMINATION OF HOLOCENE LAVAS

YEWUBINESH BEKELE REBA

Enschede, The Netherlands, February, 2016

Thesis submitted to the Faculty of Geo-Information Science and Earth Observation of the University of Twente in partial fulfilment of the requirements for the degree of Master of Science in Geo-information Science and Earth Observation.

Specialization: Applied Earth Sciences

SUPERVISORS:

Dr. C.A. (Chris) Hecker

Dr. F.J.A. (Frank) van Ruitenbeek

THESIS ASSESSMENT BOARD:

Prof. Dr. F.D. (Freek) van der Meer (Chair)

Dr. Friedrich Kuehn, Federal Institute for Geosciences and Natural Resources (BGR), Germany

DISCLAIMER

This document describes work undertaken as part of a programme of study at the Faculty of Geo-Information Science and Earth Observation of the University of Twente. All views and opinions expressed therein remain the sole responsibility of the author, and do not necessarily represent those of the Faculty.

ABSTRACT

An assessment of the reflectance spectra of obsidians as a possible tool for dating of different Holocene lava flows from the southern Main Ethiopian Rift (MER) (Ethiopia) active volcanoes is described. Rock samples from obsidian lava flows of different ages were collected from four volcanic regions namely TulluMoje, Alutu, Corbetti and KorkeSelewa. Rock samples were collected from obsidian lava flows which are not covered by vegetation, soil or pumice fall.

The reflectance spectra of 38 rock samples were measured in the range of 350nm to 2500nm using ASD Fieldspec Pro spectrometer while the thermal infrared (TIR) spectra were recorded from 1700 - 16000nm for 8 of the rock samples using Bruker Vertex 70 spectrometer. Complementary XRD analysis was done to correlate and interpret the SWIR reflectance spectra. Spectroscopy and XRD were done on both weathered and fresh surfaces of same rock sample. The inside measurements of rock samples represent the original or fresh surface while the top measurements represent the weathered rock surface. Relative geochronological sequence of eruptions in the area was obtained from published studies. 5 rock samples were measured by OSL dating technique in order to make the relative chronology in an absolute dating and evaluate the reflectance response to increasing age. The spectral depth parameters of the H₂O (at ~1900nm) and the 2200nm Al-OH absorption features presume to increase with weathering processes that results in formation or hydration of minerals, consequently increases the overall brightness of the rock samples.

The laboratory spectroscopic analyses, supported by limited XRD analyses, showed the relationship between reflectance spectra of rock surfaces and age of rock samples. The information derived from reflectance spectra (brightness) values of rock surfaces was used to compare the rock samples with respect to their age. Analysed rocks vary in age such as those dating from historical flows 1900 AD and 1775 AD flows (Tullu Moje volcanic region), flows with relative geochronology (Corbetti volcanic regions) and undated flows. The overall brightness of the rock samples, in the SWIR, seems to be controlled by weathering that causes formation/hydration of minerals. The variation in texture of rock surfaces results from the presence of phenocrysts and subsequent surface weathering (hydration) of the rocks. Both lead to variations in reflectance spectra of rock surfaces. The reflectance spectra in the SWIR (~1850nm and ~2140nm) increases with the absorption features depth (~1900nm of the H₂O and ~2200nm of the OH respectively) on weathered rock surfaces. This indicates the change in reflectance spectra of the rock samples is caused by weathering products attributed to hydration of the glass. The absorption features depth is subdued for young rock samples and increase in older rocks which correspond to their reflectance spectra. Generally porphyritic rock samples have higher feature depth and hence higher reflectance than aphenetic samples (optically different) suggests that correlation of rock samples from the two textures should be done carefully. An identical optical property on fresh surfaces (similarity of the curves in absorption features, no defined trend on the unweathered surfaces with age) suggests that all the differences observed from satellite images seems to be related to the age. As a starting point, taking the reflectance (brightness) at 1800nm was indicative of some link of the reflectance spectra of obsidian with age ($R=0.747$). Although partly qualitative, the emittance at 3.036 microns also suggests the possibility to estimate the age of the lava flows ($R= 0.884$).

The brightness in the SWIR (1800nm) is applied to ASTER imagery of lava surfaces of the study area. No correlation between the brightness (~1650nm) versus NDVI values suggests vegetation density is not a dominant factor for brightness variation at least for the sampling locations of the obsidian flows. ASTER data comparison also shows a good age-related trend. The brightness (~1650nm) increases as lava ages for the sample locations.

Although this technique is far from complete, there is an indication that the reflectance spectra (brightness) from obsidians can be used for dating of lava flows although there are some limitations of the technique that needs further investigation. This study induces many applications in the future. Although the relation between the ages and the spectra is valid only in limited areas, such a relation, even in a limited area, that can help people to do mapping and avoid hazards.

Keywords: reflectance spectra, obsidian rocks, surfaces, dating, Holocene, hydration, ASTER

ACKNOWLEDGEMENTS

Firstly, praise be to the almighty God, without his mercy and support, this study could never have been achieved. The Netherlands Fellowship program (NFP) for granting in completion of the MSc programme is highly appreciated.

I am heartily thankful to my supervisors C.A. (Chris) Hecker and F.J.A. (Frank) Van Ruitenbeek for their scientific guidance and fruitful discussion enabling me to shape my ideas and think in a scientific way. Chris, thanks for your consistent follow up and help during the ASD and TIR measurements.

Prof. Dr. F.D. (Freek) vander Meer, your comment at the last minutes added a lot to shape up the thesis writing.

I am also grateful to Vladislav Rappich, external supervisor, Czech Geological Survey for providing information current state - of - the - art knowledge on the study area, sharing his experience about the volcanoes under study and critical comments and guidance during the research.

Special and deep gratitude is also due to Viljo Kuosmanen, Geological Survey of Finland, who always encourages my thoughts and shares his scientific experience. Viljo, your constructive comments and guidance for this piece of work has significantly improved the thesis. Your encouragement words always remain in my heart.

I also thank to Long Li, Department of Geography, Vrije Universiteit Brussel, for his critical comments and scientific feedbacks.

My grateful further goes to Tsegaye Abebe for your scientific explanations of the studied volcanoes and feedbacks. My special thanks is also to Daniele Giordano, Earth Sciences Department University of Torino, helping me to get the absolute ages in OSL dating. Daniele, special thanks to take your time and measure the OSL samples during your stay in Brazil.

Special thanks to Professor Andre Oliveira Sawakuchi Andre and his groups, Luminescence and Gamma Spectrometry Laboratory – LEGaL Instituto de Geociências - Universidade de São Paulo Rua do Lago, 562 - São Paulo - SP - Brasil - 05508-080, to allow his lab to measure the OSL dates.

I am also grateful to Dr. Caroline for the XRD work and Mr. Watse Siderius for facilitating the spectroscopy work.

My gratitude is also to staff members of the Applied Earth Sciences department for their support in my study in a number of ways, Harald van der werff, Ms. Theresa and Bart Krol for their valuable contributions at particular stages of my study.

Finally, my greatest thanks go to my family: mom, dad, my sisters and brothers for their love and encouragement during my study. My brother (Yenukab) you are always by my side when I need your help.

TABLE OF CONTENTS

Contents

1.	Introduction.....	1
1.1.	Research Background	1
1.2.	Statement of the problem	1
1.3.	Motivation.....	2
1.4.	Objectives of the study.....	2
1.5.	Research Questions.....	2
1.6.	Hypothesis	2
1.7.	Data sets.....	2
1.7.1.	Rock samples and spectral data	2
1.7.2.	Eruption dating	3
1.7.3.	Remote sensing data.....	3
1.7.4.	Other data sets.....	3
1.8.	Study area.....	3
1.9.	Thesis structure.....	5
2.	LITERATURE	5
2.1.	Regional geology.....	5
2.2.	Properties of natural glasses special emphasis on obsidians.....	7
2.3.	Weathering of obsidian.....	8
2.4.	Dating of volcanic rocks	8
2.4.1.	Optically stimulated luminescence (OSL) and its application in volcanic glass.....	8
2.4.2.	Spectroscopic dating.....	9
2.5.	Surface roughness and lava spectra	9
2.6.	Spectroscopy and spectral detectable absorption features.....	9
3.	METHODOLOGY	11
3.1.	Introduction	11
3.2.	Fieldwork and sample material	11
3.3.	Spectroscopic methods.....	15
3.3.1.	ASD Spectroscopy (VIS-SWIR).....	15
3.3.2.	Thermal Infrared Spectroscopy (TIR).....	15
3.3.3.	Spectral analysis and interpretation.....	16
3.4.	X-ray diffraction (XRD) analysis	17
3.5.	Optically stimulated luminescence (OSL) dating.....	18
3.6.	Data analysis	18
3.6.1.	Spectral Indices.....	18
3.7.	Comparison of laboratory spectra with image spectra	18
4.	RESULTS	19
4.1.	Spectroscopy	19
4.1.1.	Spectral reflectance of rock surfaces.....	19
4.1.2.	TIR spectra of rock samples	25
4.1.3.	Mineralogical features in the VIS-SWIR spectra of rock samples	28
4.1.4.	VIS-SWIR absorption features of rock samples.....	29
4.2.	XRD analysis of rock samples	30
4.3.	OSL ages of rocks samples	30
4.4.	Spectral Indices	31

4.5.	ASTER: Reflectance comparison (extrapolation).....	37
5.	Discussion.....	40
5.1.	Discussion.....	40
5.2.	Age-related variations in SWIR-TIR spectra of rock samples	40
5.3.	Spectral indices and their relation to average brightness of rock samples	41
5.4.	Can XRD reveal mineralogical information in the weathered and unweathered surfaces in obsidians?	41
5.5.	Is there any link between average brightness and relative ages in the Corbetti and Tullu Moje volcanic regions?.....	41
5.6.	Is there a link between average brightness and absolute age dating?	42
5.7.	Interpretation of the ASTER observations	42
6.	CONCLUSIONs and recommendations	42
6.1.	Cconclusions	42
6.2.	Recommendation	44
6.3.	Limitations of the technique (reflectance spectra of obsidians as a tool for age determination).....	44

LIST OF FIGURES

FIGURE 1: (A) AN OVERVIEW MAP OF THE FOUR VOLCANIC AREAS WITHIN THE MAIN ETHIOPIAN RIFT (MER)	4
FIGURE 2: GEOLOGICAL SKETCH MAP OF THE MAIN ETHIOPIAN RIFT IN THE QUATERNARY SHOWING MAJOR STRUCTURES AND FAULTS. 6	6
FIGURE 3: FLOW CHART OF THE RESEARCH METHODOLOGY	11
FIGURE 4: SAMPLE LOCATIONS IN THE STUDIED VOLCANIC REGIONS.	12
FIGURE 5 ILLUSTRATION OF THE OUTCROPS IN THE THREE VOLCANIC REGIONS:	14
FIGURE 6: GEOLOGICAL SKETCH-MAP OF THE CORBETTI VOLCANIC SYSTEM.....	14
FIGURE 7: ILLUSTRATION OF THE LAB ASD MEASUREMENTS OF WEATHERED AND UNWEATHERED OF ROCK SAMPLES.....	16
FIGURE 8: ILLUSTRATION SAMPLE PREPARATION STRATEGY FOR THE WEATHERED AND UN-WEATHERED ROCKS' SURFACES	17
FIGURE 9: LABORATORY REFLECTANCE SPECTRA OF ROCK SAMPLES FROM OBSIDIAN LAVA FLOWS IN SOUTHERN MER.....	21
FIGURE 10: LABORATORY REFLECTANCE SPECTRA FOR SELECTED ROCK SAMPLES.....	23
FIGURE 11: WEATHERED AND UNWEATHERED SURFACE REFLECTANCE SPECTRA	24
FIGURE 12: LABORATORY EMISSIVITY SPECTRA FOR SELECTED ROCK SAMPLES	27
FIGURE 13: THE MAIN SPECTRAL DIAGNOSTIC FEATURES OF PHYLOSILICATES (ILLITE)	29
FIGURE 14: POWDER X-RAY DIFFRACTION PATTERN OF SELECTED SAMPLE	30
FIGURE 15: SCATTER PLOTS OF THE REFLECTANCE OF ROCK SAMPLES AGAINST THE DIFFERENT INDICES	34
FIGURE 16: LABORATORY AVERAGE REFLECTANCE SPECTRA OF ROCK:-	35
FIGURE 17: SCATTER PLOT OF THE AGE OF ROCK SAMPLES AGAINST THEIR REFLECTANCE SPECTRA (BRIGHTNESS).	36
FIGURE 18: SCATTER PLOT OF THE AGE OF ROCK SAMPLES AGAINST THEIR EMITTANCE	37
FIGURE 19: LOCATION SHOWING WEHRE THE NDVI VALUES EXTRACTED.....	38
FIGURE 20 : SCATTER PLOT OF THE REFLECTANCE AT 1650NM IN ASTER IMAGE OF TARGET REGIONS AGAINST NDVI VALUES.	39
FIGURE 21: REFLECTANCE AT 1650NM OF ASTER BANDS VERSUS RELATIVE AGES OF LAVA FLOWS.	39

LIST OF TABLES

TABLE 1: SPECTRAL BANDS AND SPATIAL RESOLUTIONS OF ASTER DATA.....	3
TABLE 2 SELECTED ROCK SAMPLES FOR THE TIR, XRD AND OSL MEASUREMENTS.....	13

LIST OF ABRIVATIONS

µm	Micrometers
A	Aphanitic
AL	Alutu volcano
ASD	Analytical Spectral Devices
CO	Corbetti volcano
I	Inside measurement/unweathered
KS	Korke Selwa volcano
MER	Main Ethiopian Rift
nm	Nanometers
OSL	Optical stimulate luminescence
p	porphyritic
ROI	Region of interest
SWIR	Short-Wave Infrared
	Top surface
T	measurement/weathred
TIR	Thermal infrared
TM	Tulu Moje volcano
TSG	The Spectral Geologist
VIS	Visible
XRD	X-ray diffraction

1. INTRODUCTION

1.1. Research Background

Absolute dating methods (i.e., K–Ar and Ar–Ar system, U–Th–Pb system and etc.) using a variety of instruments have long been used for determining exact ages of lava - effusion events. The use of these methods is time-consuming, costly and is not suitable for inaccessible areas; in addition, some lava flows are too young to date using a method like Potassium-Argon method.

In many volcanic areas, it has been proven that subaerial weathering accompanied by chemical and physical changes can be used to estimate relative ages of flows using remote sensing techniques which in turn reduces time and cost factors (Kahle et al., 1988; Abrams et al., 1991). The southern Main Ethiopian Rift (MER), which is the main focus area, is characterized by the presence of several obsidian lavas. Variability in reflectance spectra is a major signature of the numerous obsidian lavas in southern MER. Very young and fresh obsidians (e.g., Chabi volcano) are characterized by low reflectance spectra (darker), whereas increasing age associated with hydration of glass leads to increased reflectance (lighter) on both Landsat TM as well as ASTER images (Rapprich et al., 2013). In Chabi volcano, Wendo Kosha pumice (400 BC) fall is post dated by four obsidian lavas indicating these lavas are younger than this age (Rapprich et al., 2016).

Vegetation growth varies on different lava surfaces. On basaltic rocks, the soil - forming processes are by orders faster, hence, vegetation growth is so rapid that lava surfaces are obscured from aerial view in very few years (200years). In contrast, soil on obsidians (rhyolitic) is forming very slowly (the chemistry is infertile) - the southern MER is a good example where we find more than 2000 years old obsidian lavas un-vegetated. Vegetation cover also depends on climatic conditions, fracturing and water saturation of rocks, slope exposure and surrounding geology (if some basalts are close, vegetation goes faster). Although vegetation cover is much more complicating things with dating, assessing simple reflectance spectra of non-vegetated obsidians would be of crucial importance towards another technique of dating of volcanic rocks.

1.2. Statement of the problem

The abundance of numerous active Holocene volcanic eruptions with numerous obsidian lavas has made the southern MER a proper research environment to volcanologists. So far, most of the volcanological studies in Ethiopia have been focussed to the Afar area due to the rapid extension and high magma production. On the other hand, Late Quaternary (Holocene) volcanoes of the southern MER are still much less intensively studied especially on age determination (Gianelli & Teklemariam, 1993). Many lavas in the area are not suitable for geochronological dating due to absence of coherent organic remnant for ^{14}C analysis, or the lack of comagmatic feldspar with glass for U-disequilibria analysis (personal communication Vladislav Rapprich, 2014).

Obsidians usually forms near the end of a volcanic cycle and are commonly linked to volcanic rock domes. Recent obsidian flows in southern MER (e.g., Corbetti volcanic system) can be considered an excellent example where obsidian flows are associated with pyroclastic deposits. Rapprich et al., (2016) noted that in the southern MER older obsidian flows seem to be brighter on satellite images than younger flows. The difference in average reflectance of obsidian flows on Landsat as well as Aster images is associated with hydration of glass (weathering process) (Rapprich et al., 2016). However rates and reasons for changing the reflectance spectra of these young obsidian lavas are poorly understood.

Thus, this research focuses on assessing the reflectance spectra of obsidians in the southern MER volcanoes that might have direct relevance for age determination of Holocene lava flows.

1.3. Motivation

Accumulations of obsidian lavas that are characterized by high absorption of light for young and fresh obsidians whereas increased reflectance (lighter shades) for older ages on Landsat as well as ASTER images is the motive to this study. Therefore, it is important to assess and systematically address if we can get absolute age by comparing optical data for lavas where we have no geochronological data. This consequently helps to do mapping and to warn the community and government of possible damages in the future.

1.4. Objectives of the study

The main objective of this research is to assess the reflectance spectra (VIS-SWIR-TIR) of obsidians to increasing ages of the silicic volcanic complexes in the southern MER, and determine ages (relative or absolute) of Holocene eruptions using the reflectance spectra from obsidian.

Specific objectives:

1. To examine the variations in spectral reflectance (optical) properties of obsidian rocks in the VIS-SWIR-TIR wavelength region in laboratory spectroscopy. Distinguishing characteristics such as the shape of the spectrum, occurrence of absorption bands in the spectrums, the change in absorption bands with albedo of a rock sample, and the change in albedo with age which are controlled by chemical composition, mineralogy, and grain size (texture) of the rock will be analysed.
2. To analyse and understand the relevant factors that changes the reflectance spectra behavior of obsidian rocks.
3. To analyse and use the reflectance spectra to estimate age.
4. To extrapolate the information and relationship to remote sensing data.

1.5. Research Questions

1. Which factors others than age (e.g. compositional differences, textural variation) influence the reflectance spectra behaviour of obsidian rocks?
2. Can we use the reflectance spectra of obsidian to estimate age? With what uncertainties? In the application and age estimation
3. Can the relationship be extrapolated to remote sensing data? Multispectral data?

1.6. Hypothesis

The hypothesis of this study is that a relationship can be established between reflectance of the surface of obsidian lava flows and their ages. There are multiple factors controlling the lava reflectance (measured in the laboratory). Age and composition are among them, but weathering (hydration of the glass) is also a very significant effect.

1.7. Data sets

1.7.1. Rock samples and spectral data

38 representative rock samples that were collected from obsidian lava flows of the four volcanic regions (i.e. Tullu Moje, Alutu, Corbetti and Korke Selwa) will be used in this research. These samples are used to study the spectroscopic characteristics of the rock samples of different ages. Additional 5 rock samples collected from the core of the block of lavas will be used to measure ages of the rock samples by optically stimulated luminescence (OSL) techniques. This age data will be used to compare the spectral responses to increasing age.

1.7.2. Eruption dating

Few eruption years are available from the literature for the study area: two historical lava flows from TulluMoje volcanic region (the 1900 AD historical observation and the 1775 AD anthropology evidenced flows) (Global Volcanism Program | Tullu Moje, 2013). 5 of the rock samples will be measured with optically stimulated luminescence (OSL) dating technique. For the Corbetti volcanic area there are relative age relationships available of overlapping lava flows as well as a single C14 carbon-14 age (400BC) for a layer Corbetti (pumice) in the lava flow stack (Rapprich et al., 2016). The few available dates are given in Appendix 4.

1.7.3. Remote sensing data

The Czech geological Survey has conducted natural hazard research in the southern MER. ASTER data has been acquired on February 5, 2006 for the area and was processed by the Czech Geological Survey during the research and this ASTER data will be used in the current research.

Table 1: Spectral bands and spatial resolutions of ASTER data. (Source: Yamaguchi et al., 1998)

Region of Spectrum	Spatial Resolution	Spectral Range (μm)	ASTER Bands
VNIR	15 m	0.25-0.60	1
		0.63-0.69	2
		0.76-0.86	band 3N(nadir looking) band 3B(backward-look)
SWIR	30 m	1.60-1.70	4
		2.145-2.185	5
		2.185-2.225	6
		2.235-2.285	7
		2.295-2.365	8
TIR	90 m	2.360-2.430	9
		8.125-8.475	10
		8.475-8.825	11
		8.925-9.275	12
		10.25-10.95	13
		10.95-11.65	14

1.7.4. Other data sets

A geological sketch-map of the Corbetti Volcanic System together with reports and shape files of the volcano's lava flows was provided and used in this study.

1.8. Study area

The study area (Figure 1) is located within the MER, Ethiopia, between the towns of Nazeret ($08^{\circ} 00'N$, $39^{\circ} 00'E$) and Arba Minch ($06^{\circ} 00'N$, $37^{\circ} 05'E$), and is an area of active volcanoes with numerous Holocene obsidian lava flows. It covers small segments of three map sheets: Nazret, Hossaina and Dila map sheets, where there are four volcanoes namely Tullu Moje, Alutu, Corbetti and Korke Selwa. In the past thousands of years several eruptions have occurred, producing numerous effusive obsidian lavas. However, due to the rapid extension and high magma production, most of the volcanological studies in Ethiopia are focused to the Afar area. On the other hand, late quaternary (Holocene) volcanoes of the southern Main Ethiopian Rift (MER) are still much less intensively studied especially on age determination. Additional information about historical lava flows of the volcanoes, along with a detail description is available on the Global Volcanism Program website (Global Volcanism Program 2013).

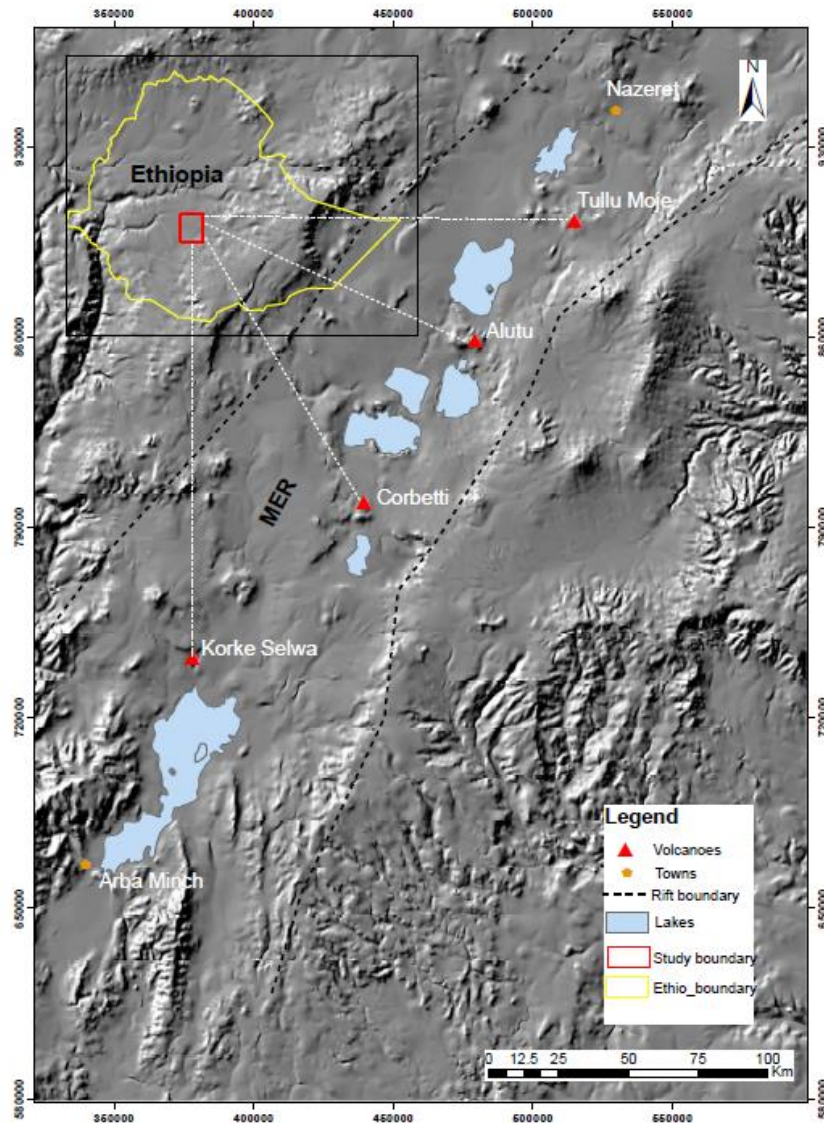


Figure 1: (a) An overview map of the four volcanic areas within the Main Ethiopian Rift (MER) ; the red triangles are the locations of the volcanoes; the volcanoes are arranged in an en-echelon fashion along the Wonji Fault Belt (WFB) in the MER.

1.9. Thesis structure

Chapter 1: Includes the research background, statement of the problem, objectives of the study, research questions, hypothesis, study area and datasets of this research.

Chapter 2: Is review of the current state - of - the - art knowledge on the study area, and other studies that were carried out such as in volcanic glasses, geochemical and spectroscopic studies.

Chapter 3: Explains the methods that were used to acquire the spectroscopic and mineralogical information, age measurement and analyse the spectral data in this research.

Chapter 4: Shows the spectroscopic, mineralogical, age measurement and ASTER: selected lava flows reflectance comparison outputs.

Chapter 5: Shows the discussion on spectroscopic, mineralogical, age measurement and ASTER: selected lava flows reflectance comparison outputs.

Chapter 6: includes summary, conclusion and recommendations based on the results.

2. LITERATURE

2.1. Regional geology

The East African Rift System (EARS) splits the continent of Africa in two. The African plate, sometimes called the Nubian plate, carries most of the continent, while the smaller Somali plate carries Horn of Africa. The EARS has western and eastern branches. The latter comprises the Ethiopian and Kenyan rifts (Abebe, 2000). The Ethiopian rift is divided into the Afar Rift (Afar Triangle), Main Ethiopian Rift (MER) and the southern (Omo – Turkana) Rift (Chorowicz, 2005).

A mantle plume that extended beneath the 1100 km wide Ethiopian plateau is responsible for the evolution of the Main Ethiopian Rift (MER) and the wide spread flood basalt volcanism and plateau uplift episodes dated at 45 – 30 Ma and 18 – 14 Ma (Trua et al , 1999). From the Afar the rift propagated from north to south. The Afar Triangle is constituted by Mio – Pliocene units of 24 to 5.4 Ma ages and Quaternary tholeiitic volcanic rocks of Quaternary age. The basement is composed of oceanic and thin continental crustal material (Chorowicz, 2005).

In the Main Ethiopian Rift (MER), volcanism started as early as the Eocene when basaltic eruption and early stage of rifting (uplift and faulting) coevally occurred (Le Turdu et al., 1999). In the southern part of the MER, volcano-tectonic activity started later than the central and northern part consistent to a north to south migration in the Ethiopian Cenozoic volcanic province Chernet, (2011), and is identified for two distinct types of volcanic systems, predominantly silicic large volcanic complexes and fields of predominantly mafic monogenetic volcanoes (Buchner et al., 2013). The volcanic activity and structural deformation of the MER has been created by a line of hundreds of young faults and volcanic centres along the rift floor and arranged in an en e´chelon fashion (WoldeGabriel et al., 1990). This volcano-tectonic axis, named the Wonji Fault Belt (WFB), is considered to be the current axis of crustal extension. The Tullu Moje, Alutu, Corbetti and Koreke Selewa volcanoes are arranged in an en e´chelon fashion along the Wonji Fault Belt (WFB)(Le Turdu et al., 1999). Korke Selewa Caldera was formed at the southern end of the MER. There are many Holecene obsidian lava flows on which this study focuses. The latest eruptions in Alutu volcanic region produced obsidian flow and pumice breccias about 2000 years ago. A regional fissure in Tullu Moje volcanic region has produced a large silicic lava flow about two centuries. Flank fissures have produced silicic obsidian lava flows as recently as about 1900 CE (Global Volcanism Program | Tullu Moje, 2013).

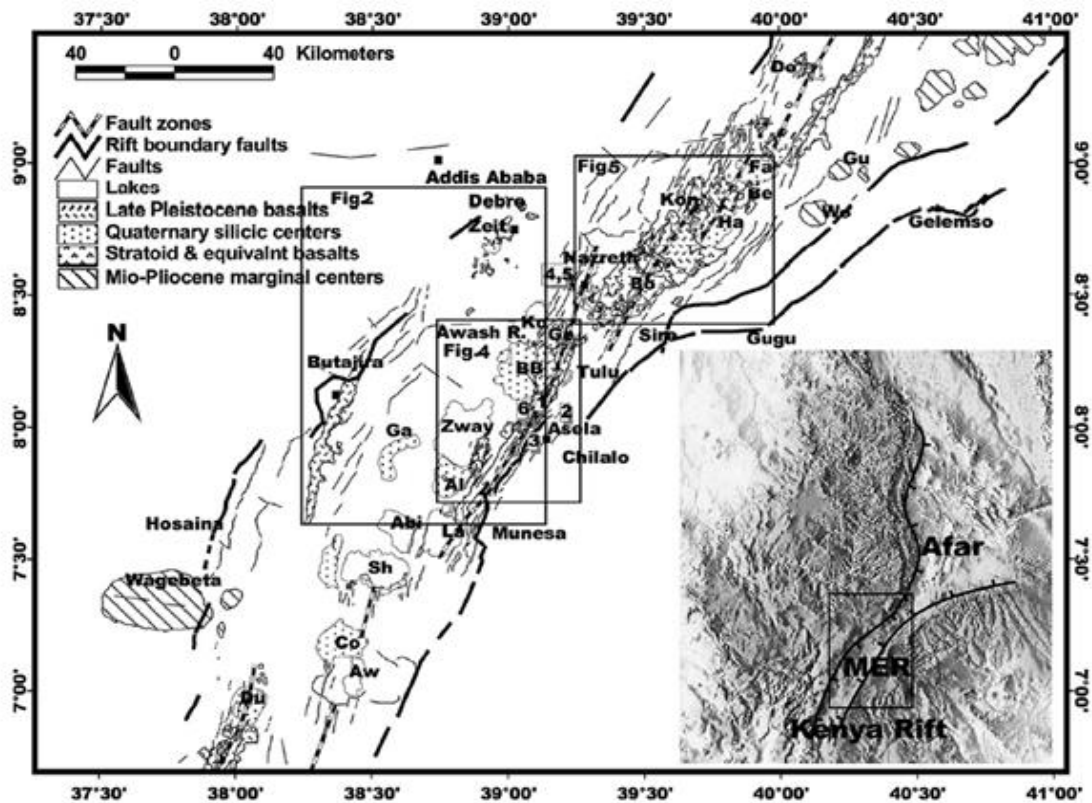


Figure 2: Geological sketch map of the Main Ethiopian Rift in the Quaternary showing major structures and faults. Inset map shows the position of the MER with respect to the red sea and Gulf of Eden. The Quaternary silicic centers are the focus of this study (Source: Abebe, 2000).

According to the Oligocene uplift of the Ethiopian plateau and subsequent generation of NE to NNE trending faults led to rifting and formation of the Main Ethiopian Rift (MER) and the southern rift. This was accompanied by fissural eruptions and the evolution of complex central volcanoes often with caldera-forming phases from rhyolitic magmas (e.g., Peccerillo et al., 2003; Biggs et al., 2011) along the rift axes. Examples of such calderas include Corbetti, Alutu and Tullu Moje for the MER and KorkeSelwa for the southern rift. The scarce intermediate rocks can be found in some volcanic systems as results of fractionation of mafic melts or mixing between mafic and silicic melts (e.g., Peccerillo et al., 2003; Hutchison et al., 2015).

The Corbetti Volcanic System is located in the central to southern part of the MER (Figure 6) and occupies NW sector of the ancestor Mid-Pleistocene Hawasa Caldera. The Corbetti caldera experienced at least three stages of devastating ignimbrite forming eruptions about 0.9, 0.67 and 0.2 Ma (JICA, 2012 and Záček et al., 2014). Two Holocene post-caldera volcanoes namely Wendo Koshe (syn. Urji) and Chabi (syn. Chabbi or Chebi) were emerged within the Late Pleistocene Corbetti Caldera and consist of accumulations of young obsidian lava flows (Di Paola, 1972; Rapprich et al., 2013), which represent a typical obsidian shield volcano. The oldest obsidians contain small phenocrysts of feldspars while the younger obsidians are pure without any crystals (Rapprich et al., 2013; Rapprich et al., 2016). The Chopa and Chabi craters represent the two episodes of explosive (phreatomagmatic) activity within the dominantly effusive Chabi Volcano (Rapprich et al., 2013; Rapprich et al., 2016). The pyroclastic sequences of the Chopa pumice cone are mostly buried by younger lavas. Fall deposited pumice alternates with flow deposits and surge deposits with associated phreatomagmatic fall and with mass-flow deposits demonstrating that some phases can be violently explosive with Plinian and phreatomagmatic eruptions (Rapprich et al., 2013). The compositional similarity as described by (Rapprich et al., 2016), makes no petrographic tool could be used to distinguish between the lava units (e.g., Chabi obsidians). Uniform chemical composition of all later eruptives of the Corbetti volcanic system has clear implications that a single common magma chamber is present to which both Wendo Koshe and Chabi volcanoes as well as all monogenetic cones are most likely attached (Rapprich et al., 2013). The rhyolitic magmas of the

recently active volcanoes within the Corbetti Volcanic System are most likely produced by extreme fractional crystallization of upper mantle-derived basaltic melts (Rapprich et al., 2016).

The rocks cropping out in the Alutu, a typical young and restless silicic volcano, are Quaternary in age and followed a period of regional basaltic fissure eruptions. The volcano underwent several large caldera-forming eruptions and developed a collapse structure (~45 km²) (Hutchison et al., 2015). Following caldera collapse several pulses of resurgent silicic volcanism have taken place, infilling the caldera and exploiting the pre-existing volcanic ring structure. The youngest products of Alutu are dated at about 2000 years (14C method) and consist mainly of obsidian flows and pumice breccias (Gianelli & Teklemariam, 1993). Geochemistry of the erupted products of Alutu shows that the youngest volcanic rocks are dominated by highly evolved peralkaline rhyolites and protracted fractional crystallisation processes were indicated by the large range in silica content and major element (e.g., Hutchison et al., 2015). The rhyolites of Alutu are characterized by a single magmatic lineage derived from parental basalt and suggest that the most evolved rhyolites of Alutu can be reached following 90 – 95% fractional crystallisation of the basalt rocks that preceded development of the complex (Hutchison et al., 2015).

Tullu Moje is one of the major felsic central volcanic complexes of Quaternary age, which rest on the sectors of the WFB at Tullu Moje hosting pyroclastic products obsidian domes and flows until recent times (Gedemsa). The center straddles on a sequence of volcanic products and lacustrine deposits of mostly Plio-Pleistocene age. The geo-volcanological studies showed the occurrence of historical volcanic flows, occurrence of phreatic explosive craters, and wide spread occurrence of altered grounds.

The Korke Selwa volcano hosts recent rhyo-obsidian flows probably representing the youngest rhyolitic activity in the area (Abebe et al., 2002). The obsidian lava pile at Selwa rises sharply to a height of 150 mts from the surrounding plain with small crater on the very top formed by the collapse of the summit. Obsidians such as the dark gray-greenish porphyritic obsidian to more greenish and less denser as well as highly vesiculated (spongy) obsidian are present in the area.

Di Paola, (1972, 1976) reported that the obsidian lavas in the Corbetti, Alutu and Tullu Moje calderas represent the latest stage of degassed and viscous volcanic eruption in the MER. They evolved after violent pyroclastic eruption(s) which formed spatially associated pumice exposures. Similarly the recent rhyo- obsidian lava flows in Korke Selwa are spatially associated with and younger in age than the Middle – Upper Quaternary pumiceous pyroclasts and recent basalts. Hence they might indicate the latest degassed and viscous volcanism episode in the area like contemporary obsidians of the Corbetti, Alutu and Tullu Moje calderas of the MER.

2.2. Properties of natural glasses special emphasis on obsidians

Glasses are best classified on the basis of either structure such as obsidian, pumice, perlite, tuff; or in combination with the composition, indicated by the name of the felsic rock of corresponding composition, such as rhyolite pumice, daciteperlite, andesite obsidian, etc. The analyses of natural glasses showed a wide range of composition (e.g., George, 2008). The published analyses range in silica content from about 40 - 82%.

Obsidians are natural glasses that are formed by rapid cooling of melted silicate. It is a volcanic acidic glassy rock related with perlite (Mrázová & Gadas, 2011). The majority of them show compositions approximating to 80% SiO₂, 10% Al₂O₃ with other major constituents being Na₂O, K₂O and FeO (Ericson et al., 1975, Liritzis & Laskaris, 2011; Rendell et al., 1985). Compared to Pyrex, it is found to be a glass of high chemical durability, and high hardness analogous with silica glass. Over along period of time, obsidian glass gradually undergoes a series of textural modifications related to high temperature crystallization (mainly feldspars and silica phases), the most prominent being the generation of a spherulitic texture. Pyroclastic and glass fragmentary volcanic rocks are usually devitrified to zeolitic and clay mineral assemblages; more rarely can undergo high temperature spherulitic devitrification (i.e. crystallization) (Lofgren, 1971; Gimeno, 2003) and references there in.

Infrared spectra and optical microscopic observations of obsidian reveal the complexity of the structure, which is correlated with the physical properties such as hardness and density. Microprobe analysis of homogenous glass of obsidian has confirmed their subalkaline, and particularly high-K calc-alkaline character (SiO₂ ≥ 70 %, Na₂O + K₂O < Al₂O₃), which is typical of rhyolitic melts Mrázová & Gadas (2011), furthermore a sharp contact between the core and the surface layer of obsidian reflects changes in the H₂O content.

XRD pattern studies from obsidians (e.g., Ericson et al., 1975; Ghasemzadeh et al., 2011) have shown the entirely amorphous character which is a non-hydrated silicate glass that have a three dimensional disordered framework structure.

2.3. Weathering of obsidian

The weathering acts up on the surface of the earth and causes even the hardest of rocks to change. Water, wind, and chemicals attack and break down a rock surface. This break down of and alteration of the earth's rocks by the earth's atmosphere is called weathering.

Unlike physical weathering, which changes only the size of the rock material, chemical weathering alters the rock chemically. A form of chemical weathering on rock e.g. oxidation can change iron to iron oxide. This change can be recognized from the colour change of the altered surface, indicating that the outer layer of the rock has undergone chemical weathering. Obsidian is an amorphous natural glass that posses some degree of spatial order (minimum crystal growth). Thus obsidian contains pristine water (H₂O) and sparse crystals of variable sizes of a few microns. This facilitates the process of hydration in obsidian that involves physicochemical changes in the glass (Anovitz et al., 2008). This specific type of weathering increases the water content with in the rock by absorbing the water with in the atmosphere by the obsidian. Consequently the surface of this rock is weathered in the atmosphere and the environmental context (Friedman & Obradovich, 1981). The weathering processes, including the hydration of obsidians, are accelerated by relatively high temperature and humid environments, where the warm conditions can facilitate a measurable hydration thickness in less than fifty years (Liritzis & Laskaris, 2011).

In a study involving the experimental alteration of obsidian, Kawano et al., (1993) showed the formation of clay minerals as reaction with distilled-deionized water progressed. This product consisted mainly of Si, Al, and small amounts of Ca, K, and Fe. The experiment revealed the formation of a dealcalized leached layer on the surface of obsidian and suggested that the formation process of smectite observed in the study seems to be one of the possible weathering processes occurring in nature.

2.4. Dating of volcanic rocks

Determining exact ages of lava - effusion events has been dependent upon K–Ar and Ar–Ar system, U–Th–Pb system, cosmogenic nuclides accumulated on surfaces, radiocarbon of intercalated organic matter, U-series disequilibrium system, fission-track geochronology, luminescence geochronology and obsidian hydration dating (OHD) (Lu & Dzurisin, 2014; Cheong, 2014). The latter technique is an alternative geochemical method to determine age in either absolute or relative terms (Friedman & Obradovich, 1981; Liritzis & Laskaris, 2011; Smoak, 2013). The above methods are costly, and are not suitable for inaccessible areas; although some lava flows are too young to date using Potassium-Argon method can be mentioned as limitation. Specific to the main focus areas of this research, the MER, the usefulness of some of the above methods are often limited by absence of coherent organic remnant for ¹⁴C analysis, lack of comagmatic feldspar with glass for U-disequilibria analysis V. Rappich (personal communication, 2014) and their young age for potassium-Argon method.

2.4.1. Optically stimulated luminescence (OSL) and its application in volcanic glass

Luminescence techniques were first attempted to date volcanic lava (Wintle., 1973) using thermoluminescence (TL). Extensive development and refinement have been made in the application for the past several years. Luminescence methods (TL and OSL) are based on evaluation of the time that has elapsed since mineral grains crystallised, were last exposed to sunlight or heated to a few hundred degrees Celsius (Preusser et al., 2008).

Currently, luminescence techniques are potentially highly useful methods for dating volcanic and related materials and events over timescales from hundred years to beyond the Quaternary. The dating protocols development in Luminescence geochronology research has been focussed on quartz and feldspar. However very recent study (e.g., Sawakuchi et al., 2015) showed the technique is promising for volcanic glasses despite the fact that much work is still to be done to develop a well-established protocol for dating of volcanic glasses G. Daniela (personal communication, 2015). For details of the applications of general luminescence dating of geological materials (not specific to volcanic glasses) and the extensive development and refinements so far, the reader is referred to a review by Fattahi & Stokes, (2003). The

approaches of luminescence usually do not possess the precision given by other absolute dating such as $^{40}\text{Ar}/^{39}\text{Ar}$ and ^{14}C methods. However it is advantageous in terms of age range and scope of material.

2.4.2. Spectroscopic dating

Imaging spectroscopy has in particular become a progressively interesting new approach to earth remote sensing (Green et al., 1998a). The quantitatively measured spectral differences of individual Hawaiian basaltic flows were used to estimate their relative ages and map with Multispectral imaging systems (Kahle et al., 1988). Previous study by Abrams et al. (1991), demonstrated the use of visible as well as reflected and thermal infrared light for the dating and mapping of Hawaiian lava flows. Factors such as oxidation of iron, development of rinds on the flows, devitrification of the thin veneer of volcanic glass, soil development and the accompanying vegetation cover were noted as a few key indicators of flow age. Another research (Walsh, 1990) on the relative dating of lava flows on Ngauruhoe, a back-arc stratovolcano, uses digital images of the mountain, and attempted to correlate spectral RGB data to the relative ages of flows. In subsequent research (Abrams et al., 1996) analysis of airborne remote sensing data and supervised classification of these data were used to determine the relative age of Etna lava flows. Analysis of a rectified satellite images of Ngauruhoe obtained from Google Earth - which tallies brightness values for red, blue, and green components of the images - suggests that flows brighten as they age (Walsh, 1990). Relative ages of obsidian lavas in southern MER were estimated from light-reflection variability from satellite images, and the lithological units relationships were later confirmed by field observations (Rappich et al., 2013). Very young and fresh obsidians in the Chabi volcano in southern MER are characterized by low reflectance spectra, whereas increasing age associated with hydration of glass leads to increased reflection on Landsat TM as well as Aster images (Rappich et al., 2016). Further application in Multispectral thermal infrared remote sensing includes the discrimination of Hawaiian basalts lava of younger than a few hundred years old that are difficult to map with visible and near-infrared images by (Crisp et al., 1990). They demonstrated that laboratory thermal infrared reflectance spectra of the exposed surface of Mauna Loa and Kilauea basalts show recognized changes with age. The quantitatively measured spectra differences of individual Hawaiian basaltic flows were used to estimate their relative ages and map with Multispectral imaging systems (Kahle et al., 1988). The technique is most diagnostic for distinguishing among sparsely vegetated flows in the region ($< 1.5\text{ka}$). An analysis that uses flows of known age to calibrate the reflectance spectra patterns observed is one of the many technical issues important in assessing relative dating of flows using satellite techniques (Walsh, 1990). Other study highlighted, the application of Light Detection and Ranging (LiDAR) intensity for the identification and mapping of different lava flows (Mazzarini et al., 2006). Elzabet et al., (2012) applied automated classification methods to Landsat data with the addition of Hyperion and ALI data to map lava flows. In this case, distinct spectral contrast between lava and vegetation contributes efficient flow mapping suggesting lava flow revegetation with time. A more recent study utilized linear spectral mixture analysis (LSMA), another potential technique, for characterizing lava flows of different age (Li et al., 2015). He used 30 m resolution Landsat Enhanced Thematic Mapper Plus (ETM+) and Advanced Land Imager (ALI) imagery in order to estimate fractions of vegetation and lava through satellite remote sensing.

2.5. Surface roughness and lava spectra

The effect of surface texture characteristics on lava spectra has been investigated in a variety of volcanic studies (e.g., Mazzarini et al., 2006; Bandfield, 2009). Texture controls rock surface porosity and will therefore influence the rate of surface weathering (Medapati et al., 2013). The more porphyritic rocks are more permeable and will therefore influence hydration. Lava surface roughness has been previously correlated with emission in the thermal infrared (Kahle et al., 1988). Peak shape in thermal infrared reflectance spectra was employed diagnostic and carefully studied which varies with surface roughness (Kahle et al., 1988).

2.6. Spectroscopy and spectral detectable absorption features

Presence of water and hydroxyl in the mineral composition play a particular role in the generation of fundamental vibrations in the TIR and their most common known overtones in the SWIR. Absorption features at $1.9\ \mu\text{m}$ are diagnostic of water bearing minerals (e.g., Kaolinite), and features at $2.2\ \mu\text{m}$ are

diagnostic of AL-OH (Clark, 1999; Amici et al., 2014). The combinations of the H–O–H bend with OH stretches contribute the absorption bands at near 1.9 μm (Green et al., 1998; van der Meer, 2004). In spectra of OH-bearing minerals, the absorption bands are determined by the OH stretch mode and the ion to which the hydroxyl is attached (Clark, 1999; Amici et al., 2014). In the TIR region (8-12 μm), sometimes known as the Si-O stretching region, fundamentals vibrational processes produces spectral features in silicate spectra (Hook et al., 1994).

Absorption-band parameters such as absorption-band position and absorption-band depth can be directly related to the structure (mineralogy) and chemistry of minerals (Clark, 1999; van der Meer, 2004). Van der Meer, (2004) proposed a simple linear approximation method of the absorption feature parameters. The relative depth, D , of the absorption feature is defined as the reflectance value at the shoulders minus the reflectance value at the absorption band minimum.(van der Meer, 2004). The depth of absorption is related to the abundance of the mineral and the grain size (Clark, 1999). Therefore the effect of hydration and presence of a minor clay phase on the rock reflectance spectra can be assessed using the 1900 nm (water) and 2200 nm absorption features.

The above two chapters provided critical background information from which the hypothesis of this research was formulated, leading to the methods to be used in this research. Therefore, the next chapter includes a brief description of the methodology used in this research project.

3. METHODOLOGY

3.1. Introduction

In this research project, spectroscopic methods were used to study the reflectance spectra of weathered and unweathered surfaces of obsidian lavas using ASD Fieldspec Pro spectrometer in the visible to shortwave infrared (VIS-SWIR) wavelength and Bruker Vertex 70 spectrometer in the thermal infrared (TIR) spectroscopy. X-ray diffraction (XRD) was used to detect and identify if there are mineral phases of the weathered and unweathered surfaces of the rock samples. Available geological map (e.g. Figure 6) and reports were used for determination of relative age of obsidian lavas from the Corbetti volcanic complex. The knowledge of the Tullu Moje volcanic complex is supported by historical eye-witnessed reports of obsidian lava eruptions, apart of existing geological map, in addition analytical ages of few lava flows from Alutu and Corbetti volcanic complexes were measured by optically stimulated luminescence (OSL). All available age data were summarized to compare and evaluate the spectroscopic response with respect to increasing ages (Figure 3).

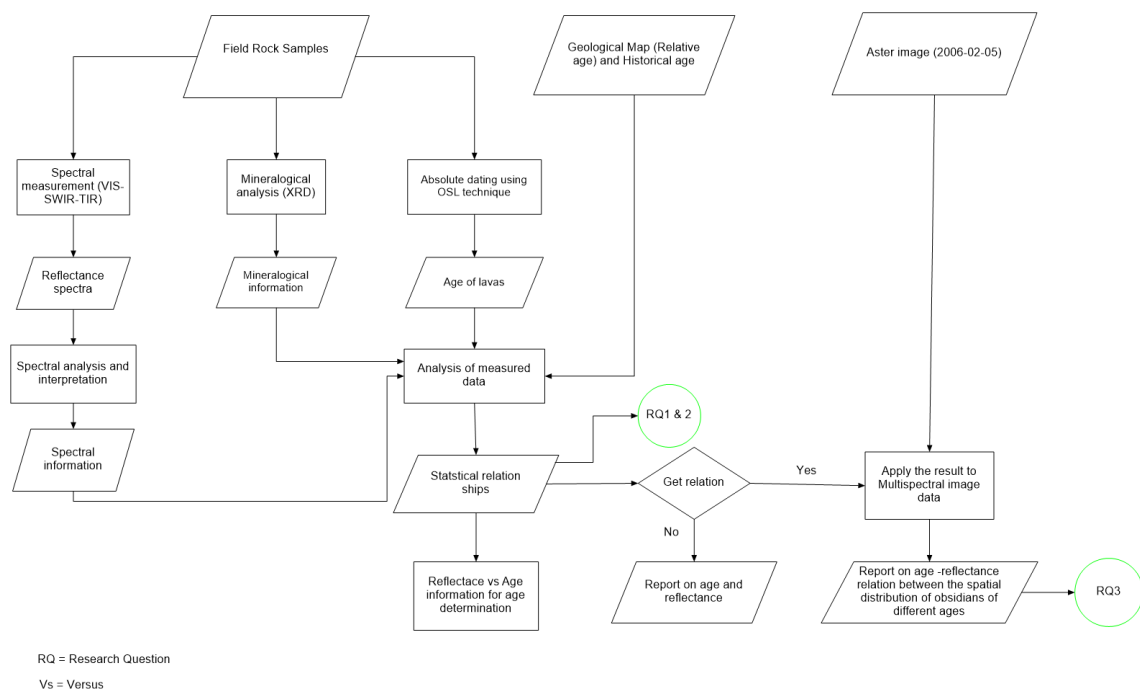


Figure 3: Flow chart of the research methodology

3.2. Fieldwork and sample material

During the field work observation was made on the outcrops. In general, the obsidian lava flows/domes are very rough, blocky and sharp (Figure 5). Tullu Moje volcanic region is composed mostly of pumice and ash with a base mostly of trachytic and rhyolitic lavas. Several craters were observed in Alutu volcanic region located at different altitudes. The region contains silicic pyroclastics such as pumice flows, pumice falls, ash and rhyolitic lava flows. The Corbetti Volcanic System shows evidence of pyroclastic eruptions followed by obsidian lavas. The WendoKoshe and Chabi Volcanoes constitute the post-caldera evolution of the Corbetti Volcanic System. In the area of Chabi Volcano, Wendo Koshe younger pumice (WKPY) covers earlier obsidians (COX–CO2) and is covered by younger obsidians (CO3–CO6) (Figure 6). The KorkeSelwa volcano hosts recent rhyo-obsidian flows and consisted green obsidian that is quite rare in the world.

38 rock samples were collected during the time Sept 2015 from traverses of four volcanic regions namely, TulluMoje, Alutu, Corbetti and KorkeSelwa and brought to ITC GeoScience Laboratory. The samples were carefully collected to select the unaltered (unweathered) and the exposed top materials (weathered) in the same sample using the smaller geologist hammer. Additional 5 rock samples were collected from deep (the core) of the block for OSL dating (big block was cut with a sledge hammer (3 – 5kg), and using the smaller geologist hammer all around the big sample (up to 5cm external part of the initial block) was scraped and only the core of the block was taken). All the rock samples are collected from obsidian lava flows which are not covered by vegetation, soil or pumice fall to avoid any non-lava pixel during comparison of the laboratory spectra with satellite spectra. Samples locations are indicated in Figure 4.

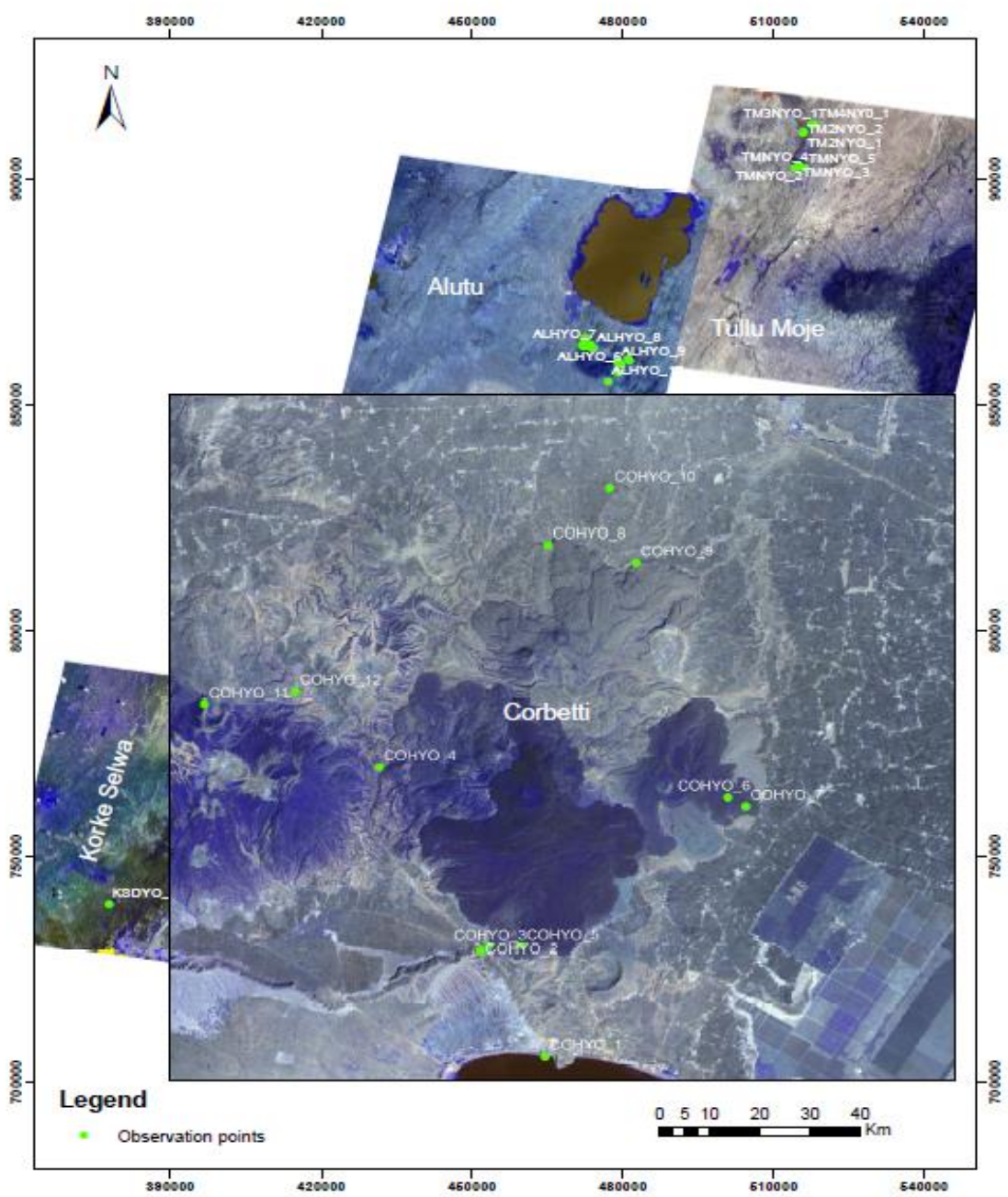


Figure 4: sample locations in the studied volcanic regions. A detailed description of these samples is given in Appendix 1.

Table 2 Selected rock samples for the TIR, XRD and OSL measurements.

Measurement	Sample_ID	Laboratory_ID	Texture
TIR	TM2NYO_1	TM2_1	Porphyritic
	ALHYO_8	AL8	Porphyritic
	ALHYO_17	AL17	Aphanitic
	COHYO_1	CO1	Porphyritic
	COHYO_4	CO4	Aphanitic
	COHYO_5	CO5	Aphanitic
	COHYO_6	CO6	Aphanitic
	COHYO_8	CO8	Aphanitic
	COHYO_10	CO10	Porphyritic
	COHYO_11	CO11	Porphyritic
XRD	TMNYO_4	TM4-1	Porphyritic
	ALHYO_11	AL11	Aphanitic
	ALHYO_12	AL12	Porphyritic
	COHYO_2	CO2	Aphanitic
OSL	ALHYO_9	AL9	Porphyritic
	ALHYO_17	AL17	Porphyritic
	COHYO_5	CO5	Porphyritic
	COHYO_6	CO6	Aphanitic
	COHYO_8	CO8	Aphanitic

TIR samples were selected based on textural variations (porphyritic vs. aphanitic), age variation were selected for the most time consuming TIR spectroscopy. Samples that show the most spectral variation for the weathered and unweathered surfaces were selected for XRD analysis as to start with and if we can see any mineralogical phases between the weathered and unweathered surfaces. Few samples are OSL samples were selected based on relative chronology data, their distribution in space and time, presence of crystals which may help dating technique, grain size, and most variations in color. Details of the samples are described in Appendix1.



Figure 5 Illustration of the outcrops in the three volcanic regions: (a) Tullu Moje volcano on the 1775 flow at location TM2_2; (b) a large view of the Alutu volcano at location AL1; and (c) The Corbetti volcano at location CO12.

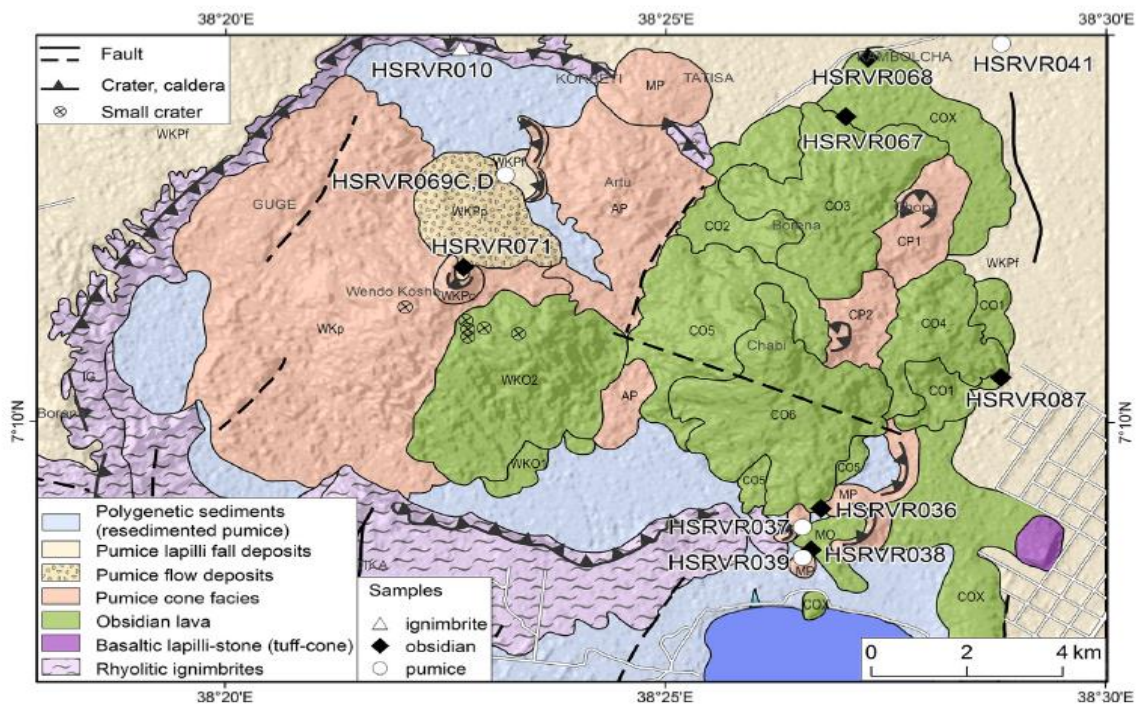


Figure 6: Geological sketch-map of the Corbetti Volcanic System. The map was used for the relative age determination. The Wendo Koshe pumice eruption (400 BC) was post-dated by four obsidian lavas. WKPF – Wendo Koshe pumice (400 BC) dominantly fall; WKPp – Wendo Koshe pumice (400 BC) dominantly flow; COX, CO1, CO2, CO3, CO4, CO5, CO6 – Chabi obsidian lavas (CO6 is the youngest). For more information on the geochronology of the Corbetti obsidian lava flows, the reader is referred to (Rapprich et al., 2016). Flows COX, CO2, CO3, CO4, CO5 and CO6 were sampled. The corresponding

sample numbers in the current study are (CO1 & CO10), CO3, (CO8 & CO9), CO6, CO2 and CO5 respectively.

3.3. Spectroscopic methods

The spectroradiometers used for collecting laboratory reflectance data include an ASD Fieldspec Pro spectrometer and Bruker Vertex 70 TIR spectrometer.

3.3.1. ASD Spectroscopy (VIS-SWIR)

Two to four measurements were taken from both the surface and the inside of each rock sample (36 rock samples) using an ASD Fieldspec Pro spectrometer in the range of 350 - 2500 μm . The ASD instrument has a spectral resolution of approximately 3 nm at around 700 nm and 10 nm at 1400 - 2100 nm. It has a sampling interval of 1.4 nm at 350 - 1050 nm and 2 nm at 1000 - 2500 nm. A contact probe of 10 mm in diameter was used directly on the sample. The locations that were measured on the sample were selected based on a flat part of the sample to ensure good contact with the contact probe as well as to get representative results in coarse samples. The ASD raw spectra files were corrected using the ViewSpecPro software (splice correction) and then converted to ASCII format files where it can be imported in to ENVI software to create a spectral library. The average spectrum of each rock sample was carefully studied using the spectral geologist and ENVI software and interpreted mainly based on the GMEX_Booklets.

3.3.2. Thermal Infrared Spectroscopy (TIR)

Thermal infrared spectra measurements were recorded for both weathered and unweathered of rock samples with the Bruker Vertex 70 TIR spectrometer with a Labsphere Infragold diffuse gold standard as a reference before each new sample. 10 of the 38 rock samples that show the most textural variations (porphyritic vs aphanitic) as well as age variation were selected and the most time consuming TIR spectroscopy was done. Spectra were recorded from 1700 - 16000 nm at a resolution of 4 cm^{-1} . A flat part of the sample is selected to ensure good contact with the sample port as much as possible. The sample port is 30 mm in diameter with a measurement spot of about 25 mm. Each sample was measured a total of eight times (without moving the sample) and averaged again to improve signal-to-noise ratio. The total measurement time for a reference and eight sample measurements was around 30 minutes. The raw Bruker spectra files were then fully processed with a dark current correction and converted to ASCII format files and imported in to ENVI software to create a spectral library. Similar to the ASD, average emissivity spectra of the rock samples was carefully studied using ENVI software and spectra of volcanic glass, obsidian and spectra of different feldspars.

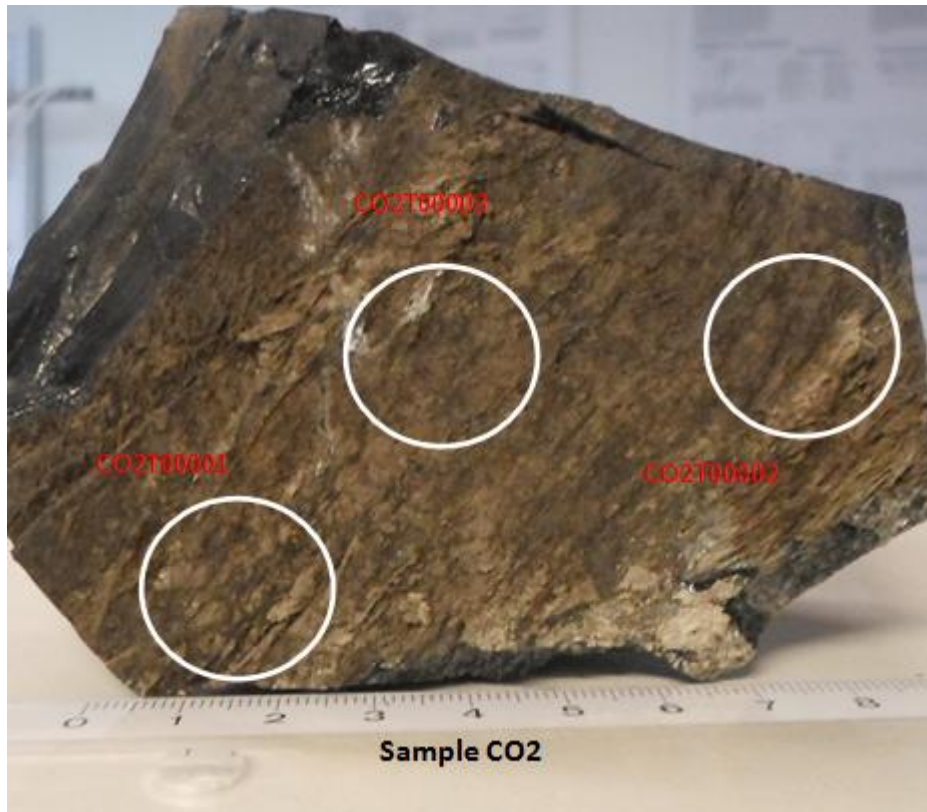


Figure 7: Illustration of the lab ASD measurements of weathered and unweathered of rock samples ; the ASD measurements were done within the white circles; the weathered surface of a vitric rock sample from obsidian lava flow from Corbetti volcanic complex (CO2) is presented as an example. Sample number is in black and spectrum numbers are in red.

3.3.3. Spectral analysis and interpretation

The spectra were analyzed and interpreted to understand the reflectance properties of the lava samples and its relation to ages (e.g. their spectral absorption feature depth that might have caused reflectance variation and hence its link to age). Visualizations of the reflectance curves and the ages were made using two softwares: The Spectral Geologist (TSG) and ENVI plot window whilst the interpretation was mainly based on the GMEX_Booklets that are associated with the TSG software. Mainly TSG software and the booklets are appropriate for the study to ease the interpretation of the low spectra of the rock samples. The comparison of the spectral curves of samples and the ages was made based on visual interpretation first and later computed mathematically. Computing of the average and standard deviation for several curves were done by spectral math in ENVI. The geometric features in the spectra increasing with increasing age were thoroughly characterized in the VIS-SWIR reflectance and LWIR-emissivity spectra curves to observe which wavelength or wavelength ranges could be linked to the lava age.

The spectral analysis was conducted using a linear interpolation technique for the hull-quotient reflectance spectrum derived by taking the ratio of the band reflectance spectrum to the enveloping upper convex Hull to quantify absorption features that are related to a certain mineral in terms of wavelength position and depth of the upper convex hull (van der Meer, 2004).

Absorption-band parameters calculated from continuum removed spectra such as the absorption-band position and absorption-band depth are used to derive compositional information on samples (van der Meer, 2004). The relative depth, D , of the absorption feature is defined as the reflectance value at the shoulders minus the reflectance value at the absorption band minimum. (van der Meer, 2004). Therefore

the effect of hydration and presence of a minor clay phase on the rock reflectance spectra can be assessed using the 1900 nm (water) and 2200 nm (AlOH) absorption features.

We also wish to investigate whether lava rock surface texture influences the spectral reflectance in the SWIR-TIR ranges. Peak shape in thermal infrared reflectance spectra of the rock samples was employed diagnostic and carefully studied which varies with surface roughness (Kahle et al., 1988).

In this study, the spectral absorption depth parameters and the overall shape of the reflectance curves in spectra with very low reflectance but still recognisable shallow composite bands, were employed to characterize variations between the weathered and unweathered surfaces of rock sample in terms of mineralogy and texture whereas the spectral depth parameter will be systematically analysed to estimate the relative hydration and/or weathering intensity of rock samples and hence age.

3.4. X-ray diffraction (XRD) analysis

In order to correlate and interpret the SWIR reflectance spectra, complementary analysis was conducted to see if XRD showed some mineralogic information for the weathered surface that was different from the inside.

Four rock samples from the two textural groups (two porphyr and two vitric) analysed with SWIR spectroscopy were selected. These samples show the most spectral variation for the weathered and unweathered surfaces. Description of the samples is given in table 2 & Appendix 5.

The samples were prepared by cutting a thin slice off the top with a rock saw (~4mm) for the top (altered) surface analysis and very unweathered part of the rock for interior (un-weathered) surface analysis (Figure 8).

The samples were then gently pulverized in an agate mortar to get homogeneous fractions. Measurements were carried out on a Bruker D2 phaser XRD diffractometer, from 5 to 70°2θ. The system utilizes a standard powder XRD setup, with the powder loaded into a sample holder that is positioned between an X-ray tube and detector.

In this research XRD analysis was mainly based on comparison of the XRD patterns, supported by other diagnostic peaks such as peaks at 21°2θ and 26°2θ can be diagnostic of the studied minerals, which are characteristic of quartz-rich acidic rocks.



Figure 8: Illustration sample preparation strategy for the weathered and un-weathered rocks' surfaces (e.g., COHYO2 aphanitic rock sample).

3.5. Optically stimulated luminescence (OSL) dating

The Optically stimulated luminescence (OSL) measurement of 5 rock samples was done in collaboration at Luminescence & Gamma Spectrometry Lab, BR-05508080 Sao Paulo, SP - Brazil. The copy of the procedures and techniques that were employed to obtain the ages by the research group is indicated in Appendix 6.

3.6. Data analysis

3.6.1. Spectral Indices

In order to link the laboratory based reflectance spectra of rock samples with rock surface weathering that results in formation or hydration of minerals, The spectral indices (properties) of two different types were tested: absorption depth at 1900 nm (H₂O feature) and absorption depth at 2200nm (OH bond/hydroxyl feature). This absorption features increase the overall brightness (albedo) of the samples attributed to weathering. In this way it seems possible that age can be measured with spectra. This can be possible ultimately by looking at the weathering which is reflected in the two spectral properties.

The reflectance values for the H₂O absorption features was taken at a shoulder value of 1850 nm while a shoulder value of 2140 nm was used for the hydroxyl (OH) feature. The two shoulder values of the H₂O and OH absorption features were used no matter that was the best shoulder for that sample or not. Illustration of the estimation of the absorption features (e.g., H₂O feature) is given in Appendix 3.

Reflectance vs. depth plots for both the 1900nm and 2200nm wavelengths were plotted for each single spectrum measured by considering shoulder values at 1850 nm and 2140 nm respectively. Point symbols were used to differentiate different groups (e.g., texture).

A single representative reflectance value for each spectrum (the reflectance at 1800 nm) was determined to show the statistics for brightness (albedo) with relative/estimated ages using a scatterplots.

By plotting the proposed spectral indices against the reflectance values at the respective shoulder, the effect of weathering on rock surface alteration/hydration and hence reflectance spectra, the effect of texture on reflectance spectra and ultimately their relation to age can be understood. Data analysis using scattergrams was employed to see the relation between the variable reflectance (e.g. as brightness) and the variable age using the weathering which is reflected in the two proposed indices.

3.7. Comparison of laboratory spectra with image spectra

ASTER is a multispectral radiometer on board Terra, the flagship satellite of NASA's Earth Observing System (EOS) launched in December 1999, capable of providing imaging information of the Earth's surface in fifteen bands- three bands in VNIR six bands in the SWIR and five bands in the TIR wavelength regions with spatial resolution of 15 m, 30 m and 90 m respectively (Abrams et al., 2015).

Multispectral sensor data of the study area that was used in this research is the Advanced Space borne Thermal Emission and Reflection Radiometer (ASTER) image acquired on February 5, 2006, freely obtained through USGS EarthExplorer site. The image was supplied as a set of georeferenced products, created by performing geometric, radiometric and atmospheric corrections on the original Level 1B image data by Czech Geological Survey. The ASTER image covers the entire area under study.

The reflectance values of ASTER were taken for the field sampling location and compared to age to see if there is still same pattern in the aster data as on the lab spectra of the samples.

The band of ASTER at 1650nm (in band 4) was selected as a proxy for overall pixel brightness which is the closest to the brightness reference point used in the lab ASD spectroscopy (i.e.1800nm). The ASTER image was exported to ENVI format with cell size 30*30 m resolution using arc map. By loading the ASTER image on ENVI a region of interest (ROI) was created for each sampling locations. Then we compute statistics for the pixels in the ROI (average spectra values).

Thereafter the reflectance at 1650nm was compared with relative ages of rock samples as well as to the Normalized Difference Vegetation Index (NDVI), to see if vegetation density is influencing the brightness at 1650nm.

4. RESULTS

4.1. Spectroscopy

4.1.1. Spectral reflectance of rock surfaces

The rocks' reflectance spectra that were examined in this study are illustrated in Figure 9. Despite the very low reflectance spectra of all rock samples, the spectral curves can be categorized into two groups based on their spectral shape and albedo. The first group includes all the measurements on porphyritic texture rock samples from historical flows (e.g., Tullu Moje volcanic complex), with relative geochronology and undated flows (e.g., Corbetti volcanic complex) and undated flows (e.g., TulluMoje, Alutu and KorkeSelewa volcanic complex) (Figure 9a). The reflectance spectra in this group are characterized by curved spectrum. The second group consists of all the vitric texture rocks from Corbetti volcanic complex (with relative geochronology and undated flows) and Alutu volcanic region undated flows (Figure 9b). The common features in the spectra were highlighted in Figure 10c & d. In the VIS range the steepest part of the reflectance curves is located at about 650 nm for the porphyritic rocks while this slope is missing in the aphanitic samples except for few samples that show distinct curve (CO2TA & CO9TA). In the NIR-SWIR, most rock surfaces' spectra show a slight increase for the porphyritic rocks while the reflectance curves are very flat for aphanitic rocks (Figure 9b dotted arrow) except for the two distinct curves. The porphyritic samples are characterised by a higher reflectance as compared to the aphanitic rock samples (Figure 11b).

A well-defined spectral feature marked by a minimum at 1900nm is observed for almost all rock samples while a second spectral feature is observed at wavelength 2200nm (Figure 10c&d). The weathered surface reflectance is higher than the unweathered surfaces reflectance (Figure 11a). Generally rock spectral signature is more pronounced in the older rocks than the younger rock sample (e.g., Figure 11b, sample CO5 < Sample CO10, relative geochronology Corbetti volcanic region).

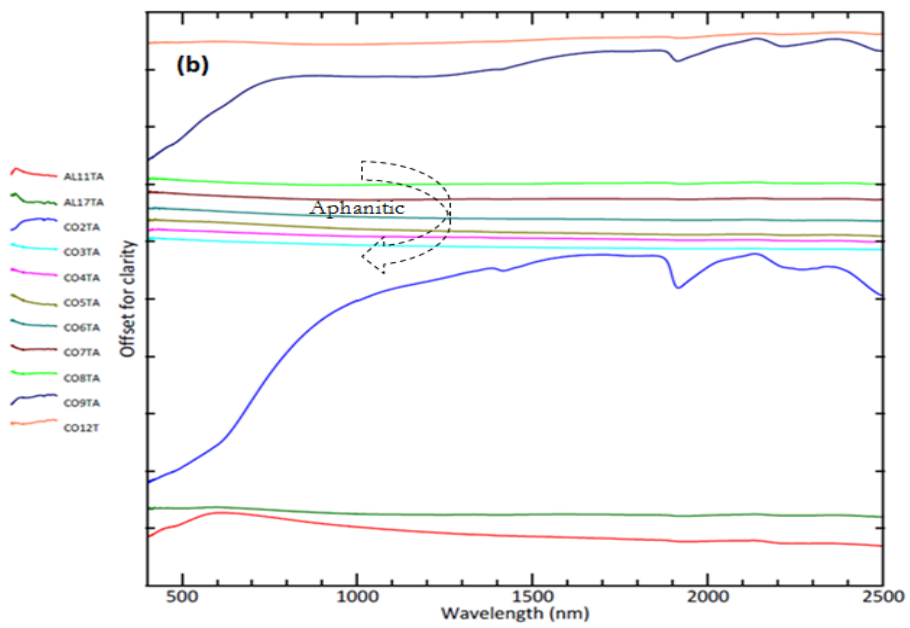
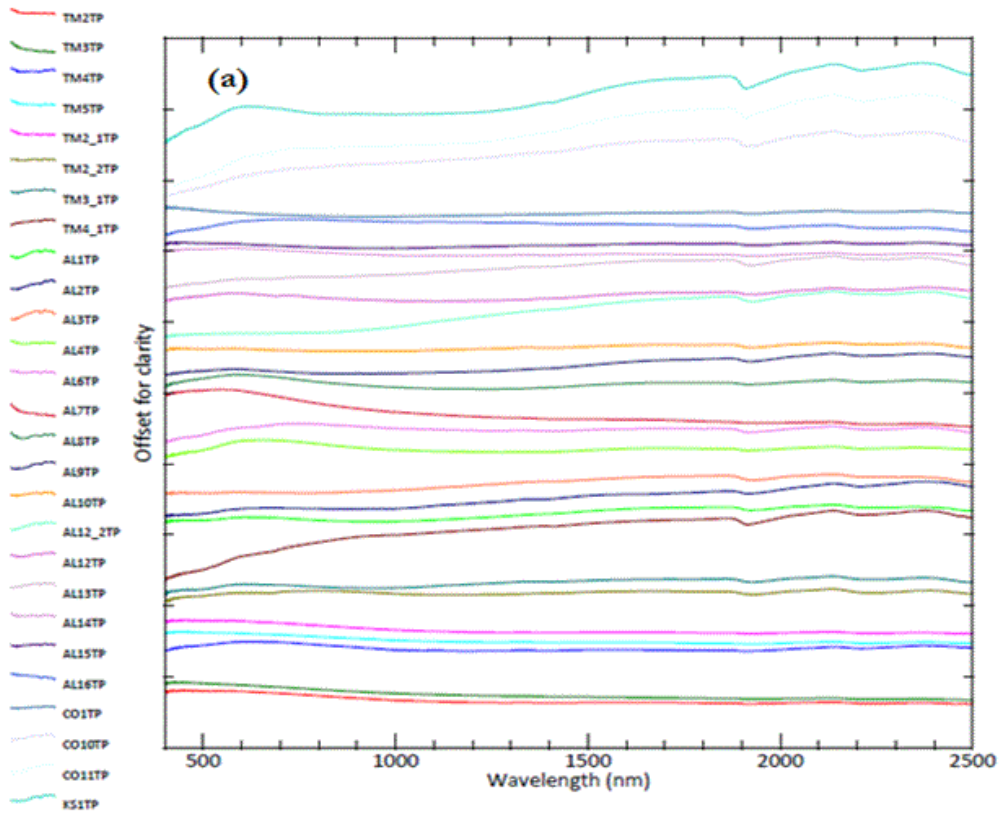
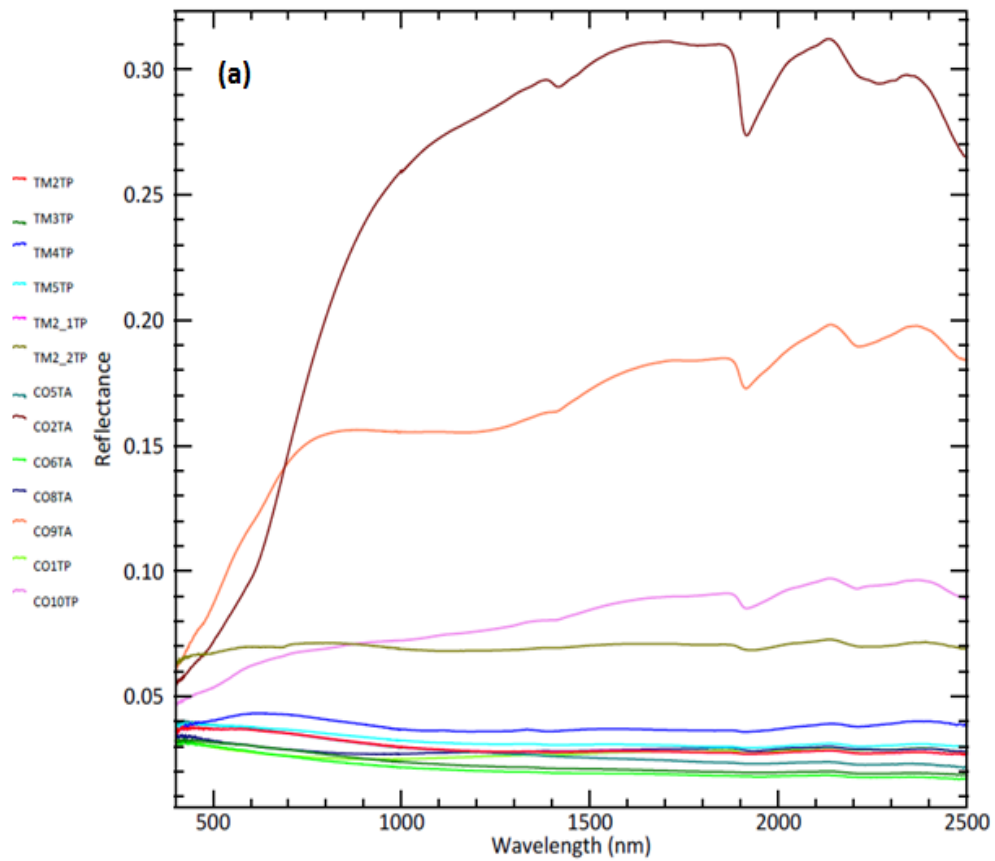
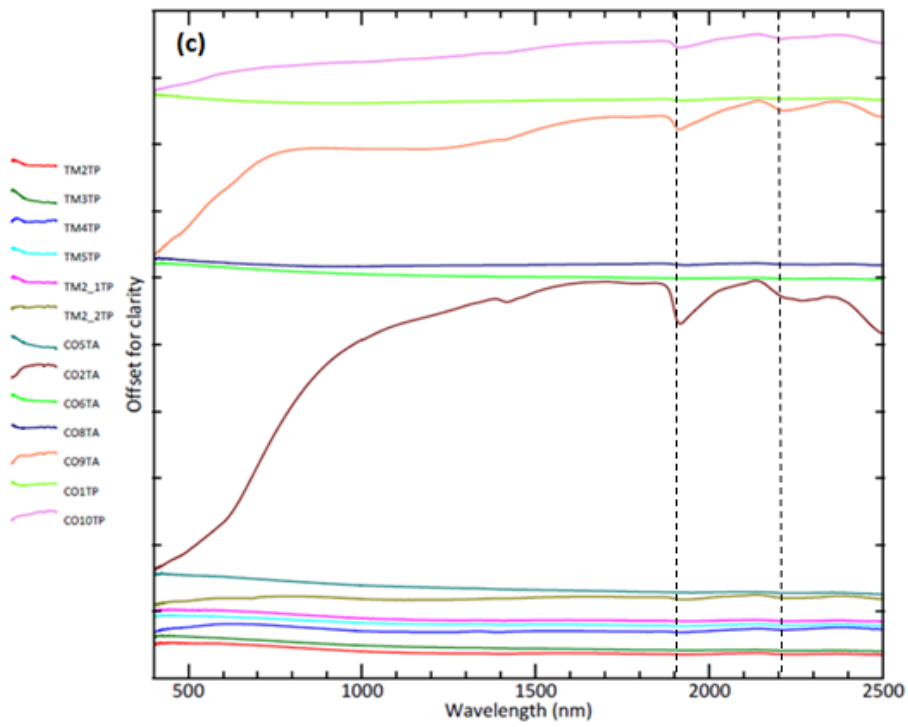
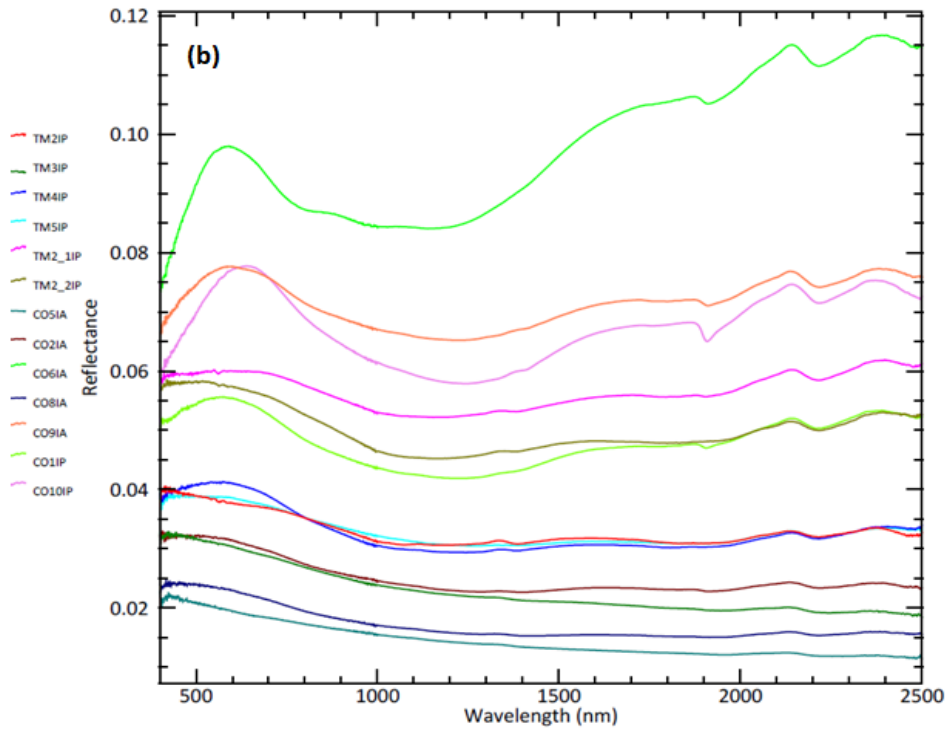


Figure 9: Laboratory reflectance spectra of rock samples from obsidian lava flows in southern MER. Each ASD curve is the average of 2-4 measurements on the weathered rock surfaces. (a) porphyritic rock samples. (b) vitric rock samples. The curves whose names (spectral number) end with a “P” or “A” were measured on porphyritic rock samples and Aphanitic rock samples, respectively. The letters before “P” or “A” stands for measurements on weathered surface “T” and measurement on unweathered surfaces “U”.





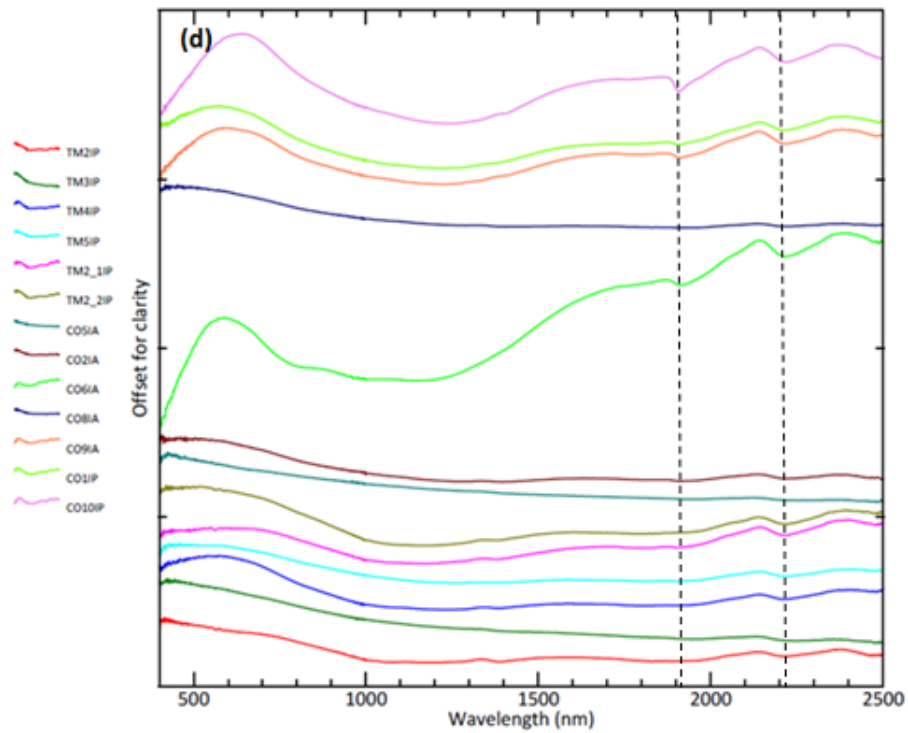


Figure 10: Laboratory reflectance spectra for selected rock samples (a) Weathered surface ASD reflectance; (b) unweathered surface ASD reflectance; (c) weathered surface ASD reflectance, offset for clarity; (d) unweathered surface ASD reflectance, offset for clarity. Wavelengths corresponding to significant spectral features are indicated by dashed lines; refer to spectral features discussed in the text. Historical age TM1(1900AD); TM2(1775AD); relative geochronology from young to old of selected samples: CO5 < CO2 < CO6 < (CO8 & CO9) < (CO1 & CO10).

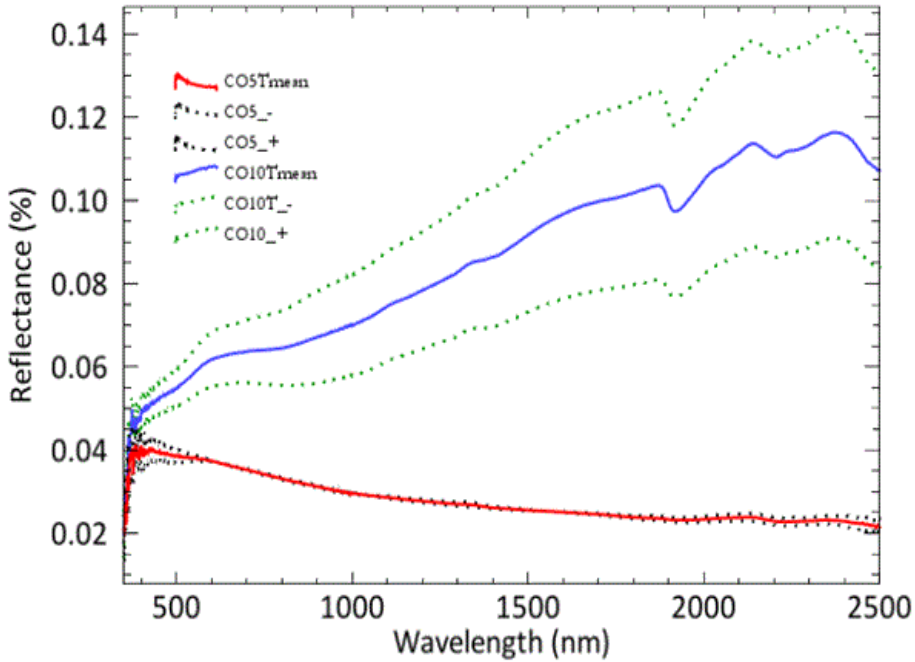
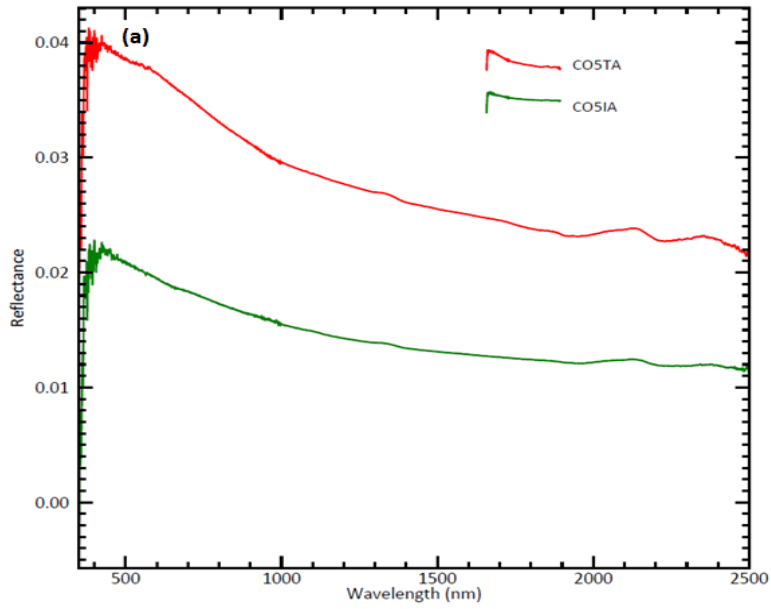
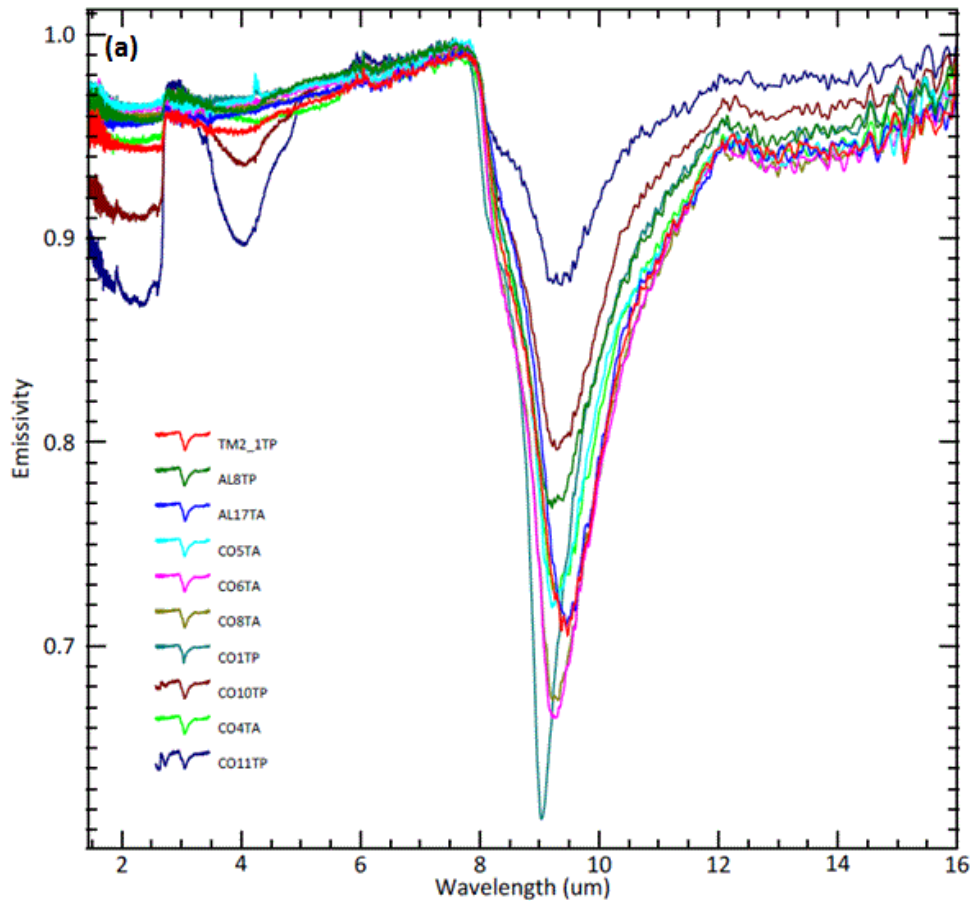
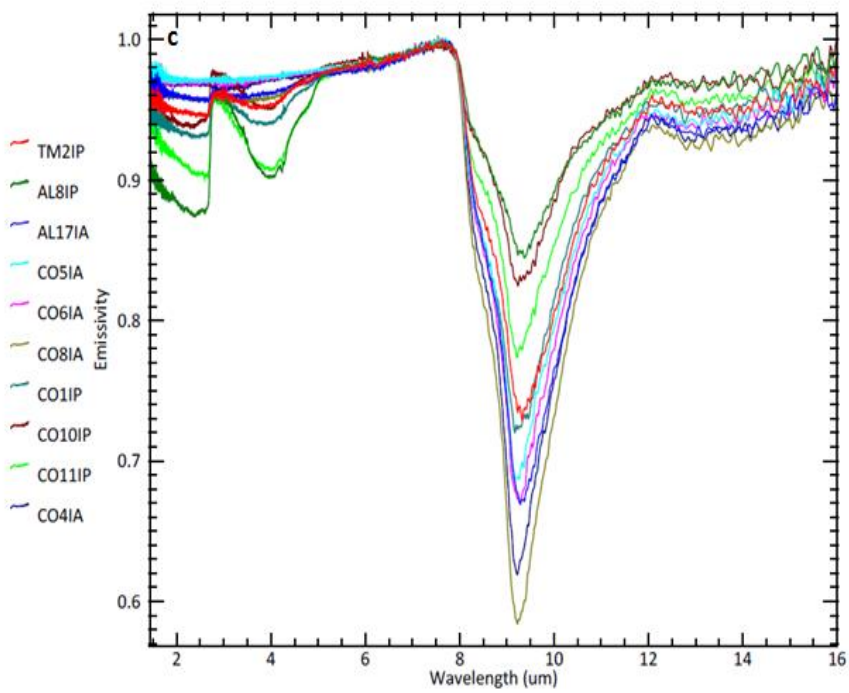
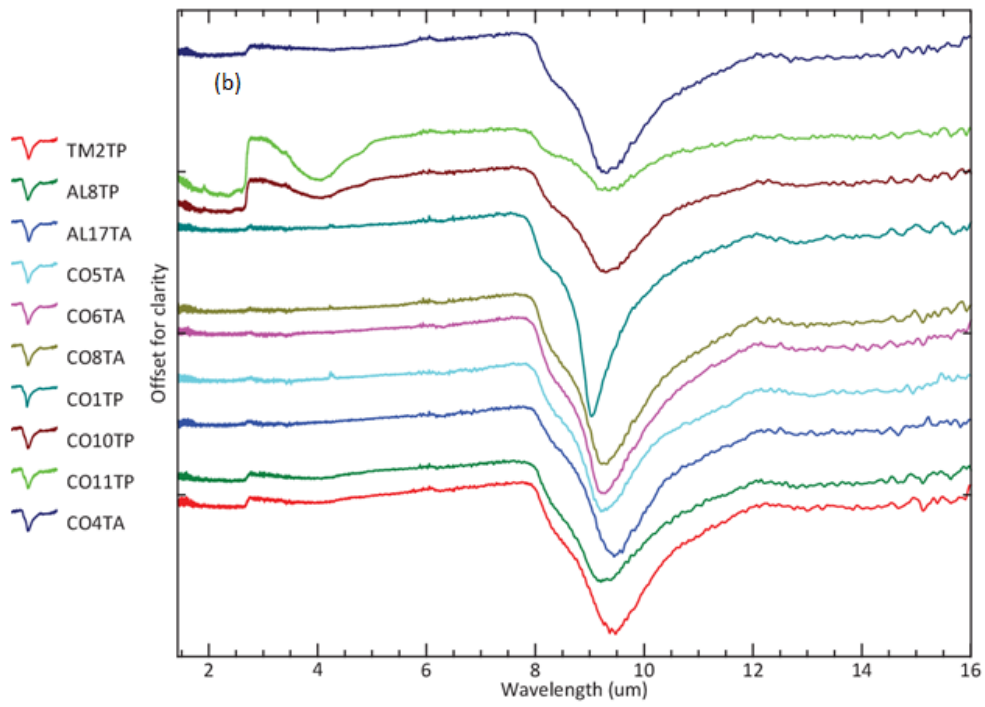


Figure 11: (a) Example weathered (CO5TA) and unweathered (CO5IA) surface reflectance spectra for rock sample CO5; (b) absolute reflectance for selected samples; dotted lines above (+) and below (-) spectral curves are standard deviations of reflectance at each wavelength for rock samples, measured from the standard deviation of the 2-4 measurement per sample.

4.1.2. TIR spectra of rock samples

Emittance spectra for the weathered and unweathered surfaces of the 10 selected rock samples are shown in Figure 12a-d. The spectra exhibit a major broad emissivity low from 8 to 12 μm and centred near 9 μm . These spectra resemble those of opal (Figure 12e). Comparison of the same sample shows that the emissivity low in Figure 12c&d (unweathered) is at a shorter wavelength (near to 9 μm) than the emissivity low in Figure 12a&b (weathered) (near 9.5 μm). The porphyritic samples with phenocrysts are characterised by more and narrower emissivity low as compared to aphanitic rock samples.





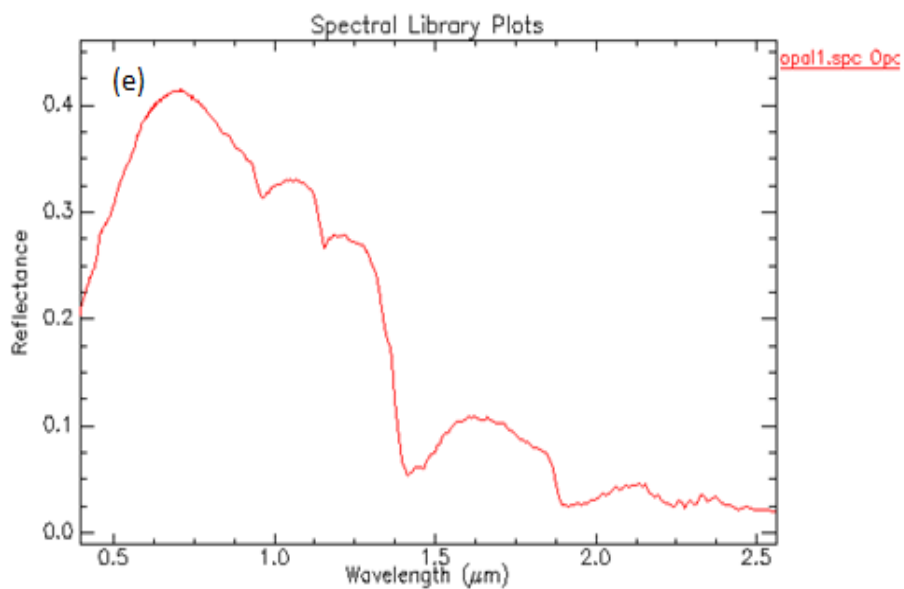
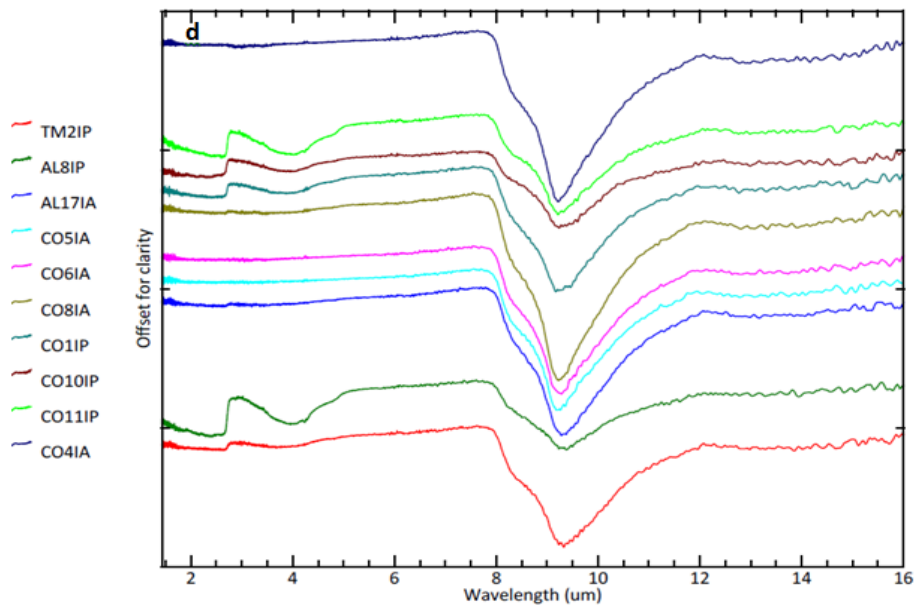
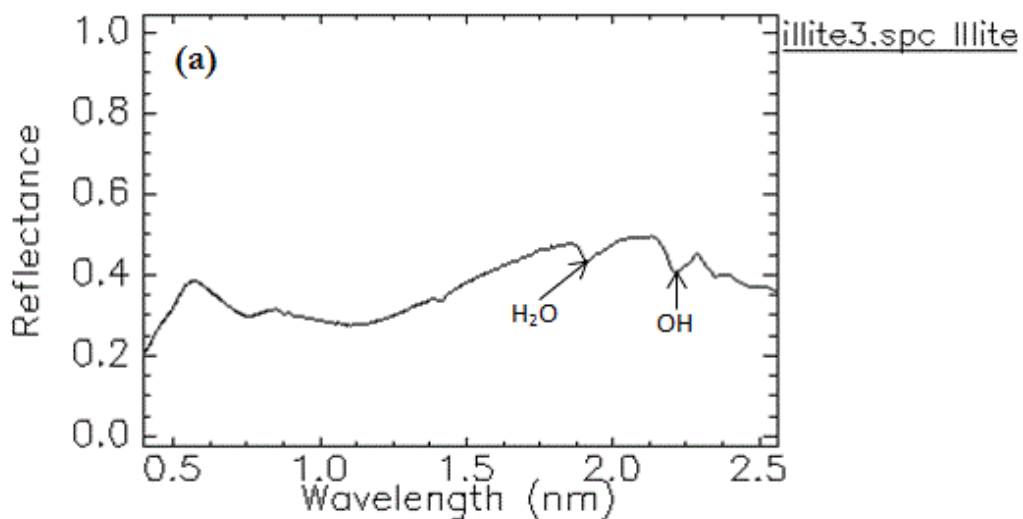


Figure 12: Laboratory emissivity spectra for selected rock samples weathered surface TIR; (b) weathered surface TIR offset for clarity; (c) unweathered surface TIR; (d) unweathered surface TIR offset for clarity. (e) opal spectra.

4.1.3. Mineralogical features in the VIS-SWIR spectra of rock samples

Even though the main scope of this research is focussed on the possibility for age determination of lava flows from reflectance spectra, analysing the mineralogy of the rock samples is important to see whether there is mineralogical variability in the rock samples that cause reflectance variation and hence age of the samples. Therefore detection of minerals in the SWIR which later be confirmed with XRD was helpful.

As a result of the spectroscopic interpretation, clay minerals most probably illite have been recognized according to the spectral absorption features that are considered as diagnostic. The Al-OH (2200nm) absorption feature was basically used to identify felsic minerals that could be present in our rock samples (Figure 13). However, due to very low samples' reflectance and which is typical of amorphous glass, minerals are difficult to identify and also to get a spectral match with the spectral library mineral spectrum. Nevertheless, Illite has a deeper absorption feature close to 1900 nm and shallower Al-OH absorption feature at nearly 2200nm (Illite-to-muscovite-crystallinity). Therefore, these absorption features can be helpful and diagnostic at least for the presence of water and some clay minerals in our rock samples.



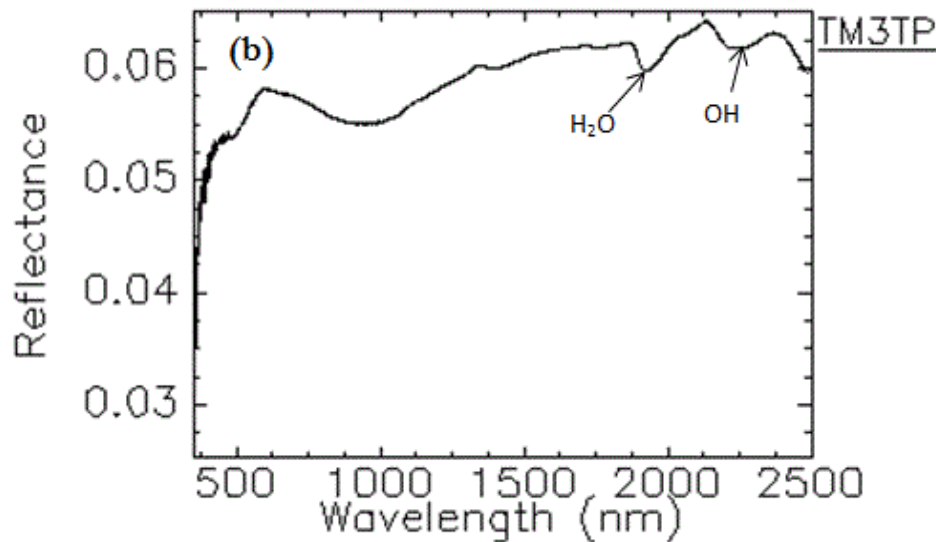


Figure 13: The main spectral diagnostic features of phyllosilicates (Illite) (a) and Sample TM3T. Spectra were compared with the USGS spectral library (Illite: illite 3.spc Illite). Arrows indicate the main diagnostic absorption features that were referred in the text.

4.1.4. VIS-SWIR absorption features of rock samples

Each of the rock samples was sampled from several lava flows indicated in Figure 9. Based on the shape of their spectral curves, we noted two main shallow features in spectra of rock samples which are common to all of the rock samples that we studied. The two features are: a band centred at near 1900 nm and a band centred near 2200nm. The ~1900nm and ~2200nm absorption features may be related to the rock (lava) samples' weathering (hydration); thus the choice of these features as an indicator for weathering (hydration) and hence cause for the reflectance variation was somewhat ideal (Figure 10).

The shape of the spectrum is indicative of porphyritic and aphanitic texture, and of weathered vs unweathered. As discussed above mineralogically there is not much information to see in the rock samples apart from the 1900nm (water) feature and 2200nm (hydroxyl) feature - most probably linked to Al-OH. Each of the two spectral features is found in the spectra of both porphyritic and aphanitic rock samples; however, spectral features of aphanitic are relatively subdued compared to those in porphyritic.

In the studied rock samples the two features are shallow developed in the spectrum, but are commonly observed together in the spectra. The 1900 nm absorption is likely due to water. But the two peaks and the absorption between them are significantly present in many of the curves. As the rocks age, the 1900 nm feature become deeper, e.g., the CO11 and CO10 rocks show spectral reflectance at ~1900 nm higher than the others, and relatively shallow 2200nm spectral feature is essentially observed. As the measurements were taken near-distance and indoors, the atmospheric water can practically be omitted.

It is evident that none of the two spectral features trend observed in the spectra of the top surfaces corresponds to the spectral features of the interior of the same rock (Figure 10a, b). This may be related to the thickness and size of samples, where the inside part of the samples normally remains fresh, unaffected by other factors. Figure 11a shows the similar curves that do not differ much for the weathered and unweathered surface. Comparison of the weathered vs. unweathered surface reflectance spectra of sample CO5 gives information about the environmental impact (hydration) on the rock surface where the weathered part of sample is characterized by relatively higher reflectance than the unweathered or fresh part of same sample (Figure 11a).

The older rock samples (CO10) show spectral reflectance at ~1900 nm higher than the others. The feature at ~ 2200nm is also higher for this older rock sample. Just like for the porphyritic rocks, the features are

distinct for aphanitic rock samples, although the later show relatively low spectral reflectance (Figure 9). In general, all rock samples' spectra show a higher reflectance across the wavelengths for the oldest rocks except sample CO2 (Figure 10).

4.2. XRD analysis of rock samples

Results of the XRD analysis are given in Appendix 5. The results from the XRD analysis revealed also information about the amorphous nature of the rock samples; hence the XRD of the selected samples does not allow calculating the mineralogical composition of samples except its amorphous volcanic glasses. The qualitative mineralogical interpretation of the spectra indicates an amorphous glass with probably some quartz and feldspars (Figure 14).

In all analysed samples, diffractograms show diagnostic peaks of quartz which is expected because of the rhyolitic composition of the rock samples (obsidians). However, samples did not show any other minerals information that could be interpreted as compositional information in XRD data and complement the presence of some clay mineral phases as seen from the SWIR analysis.

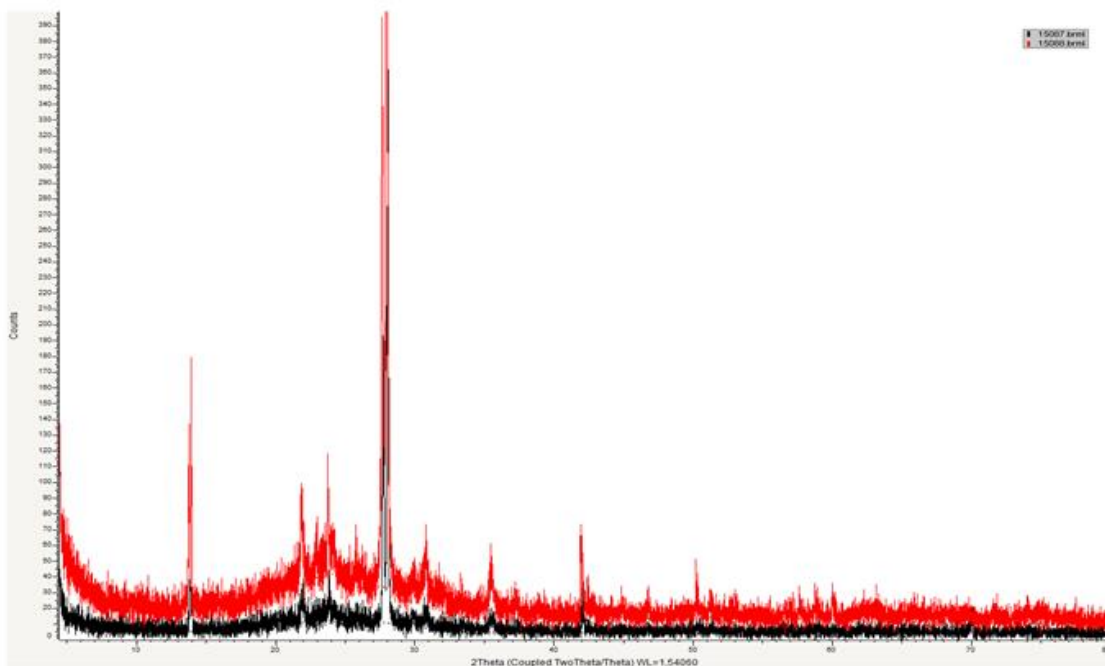


Figure 14: Powder X-ray diffraction pattern of selected sample (e.g. TM4_1) for the weathered (black) and unweathered (red) surface showing the typical of amorphous spectra of volcanic glass.

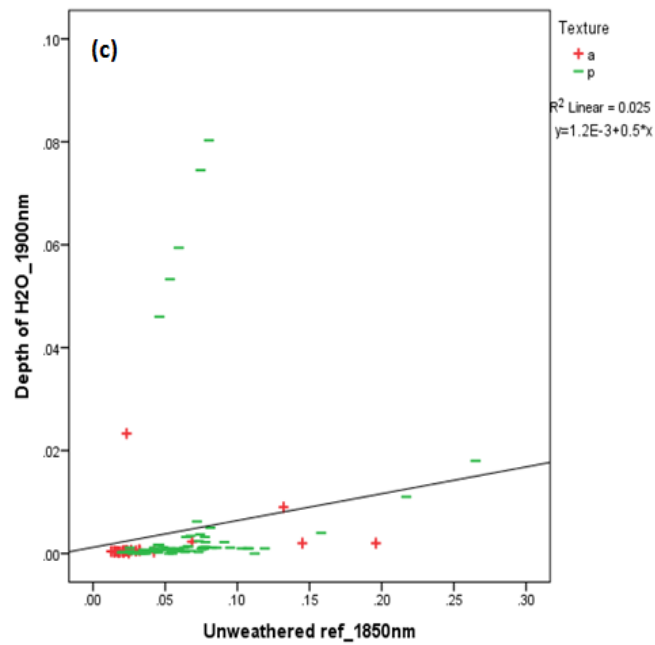
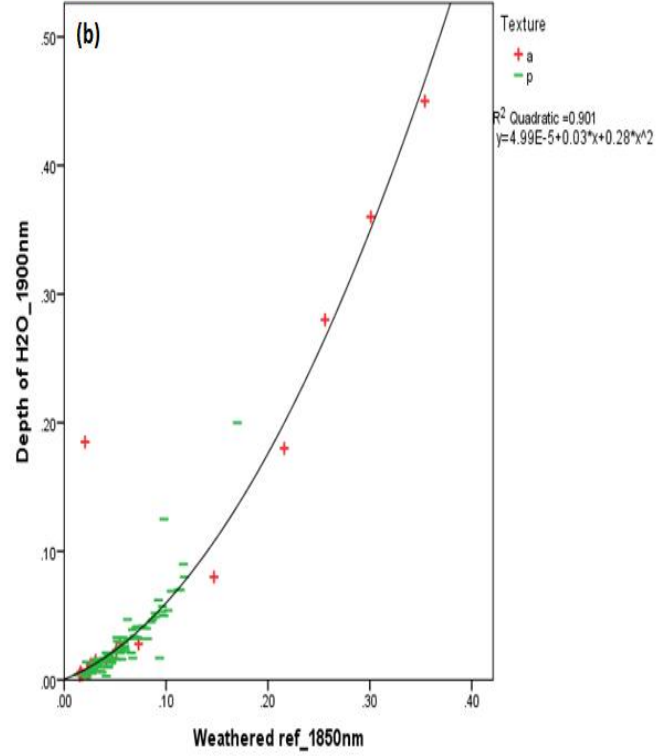
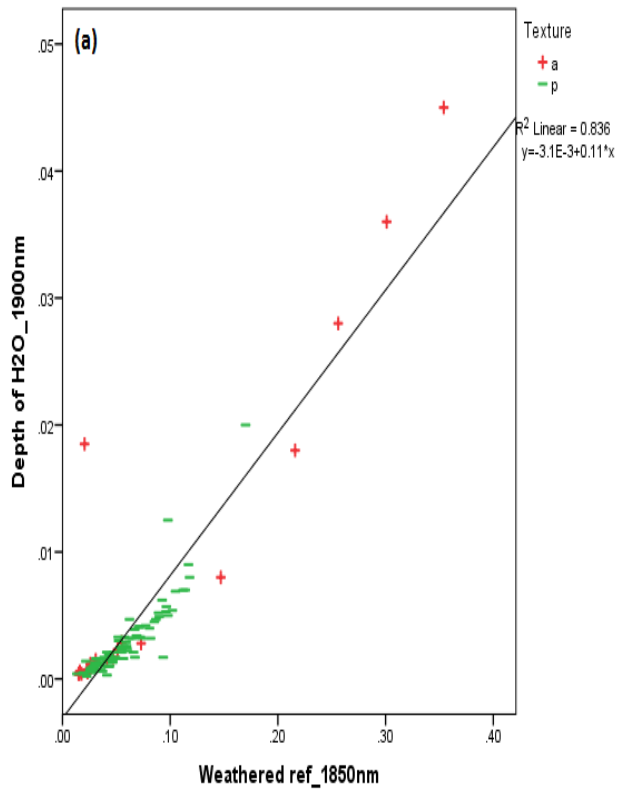
4.3. OSL ages of rocks samples

The measured OSL ages of the rock samples and comments on the result by the research group at Luminescence & Gamma Spectrometry Lab, BR-05508080 Sao Paulo, SP – Brazil are indicated in Appendix 7. Some of the OSL measured ages have high margin of error and others low. This could happen because dating of volcanic glass is still challenging. It's promising, but not straightforward so far. Luminescence dating is well established for quartz and potassium feldspar only. In luminescence dating, each sample can have a particular behaviour. The OSL ages can be considered as preliminary, but supporting a look forward to keep working on this. The data is new for the area, which is a good point. The OSL data didn't solve all geochronological problems, but opened a new perspective for future investigation.

4.4. Spectral Indices

Based on the spectral signatures of weathered and unweathered rock surfaces, we considered the depth at the 1900 nm and 2200 nm, corresponding to the H₂O and OH absorptions, defining the hydration and crystallinity.

Linear relationships between the two depth parameters and reflectance were analyzed for the weathered surface. The linear relationship suggests that the depth of the water feature depends on the brightness of the sample (Figure 15), although it is difficult to directly quantify the hydration and/or weathering from chemical analysis.



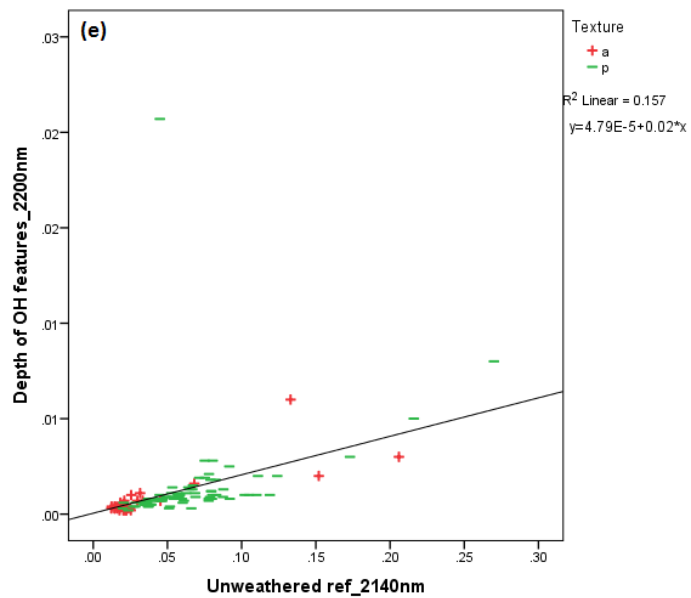
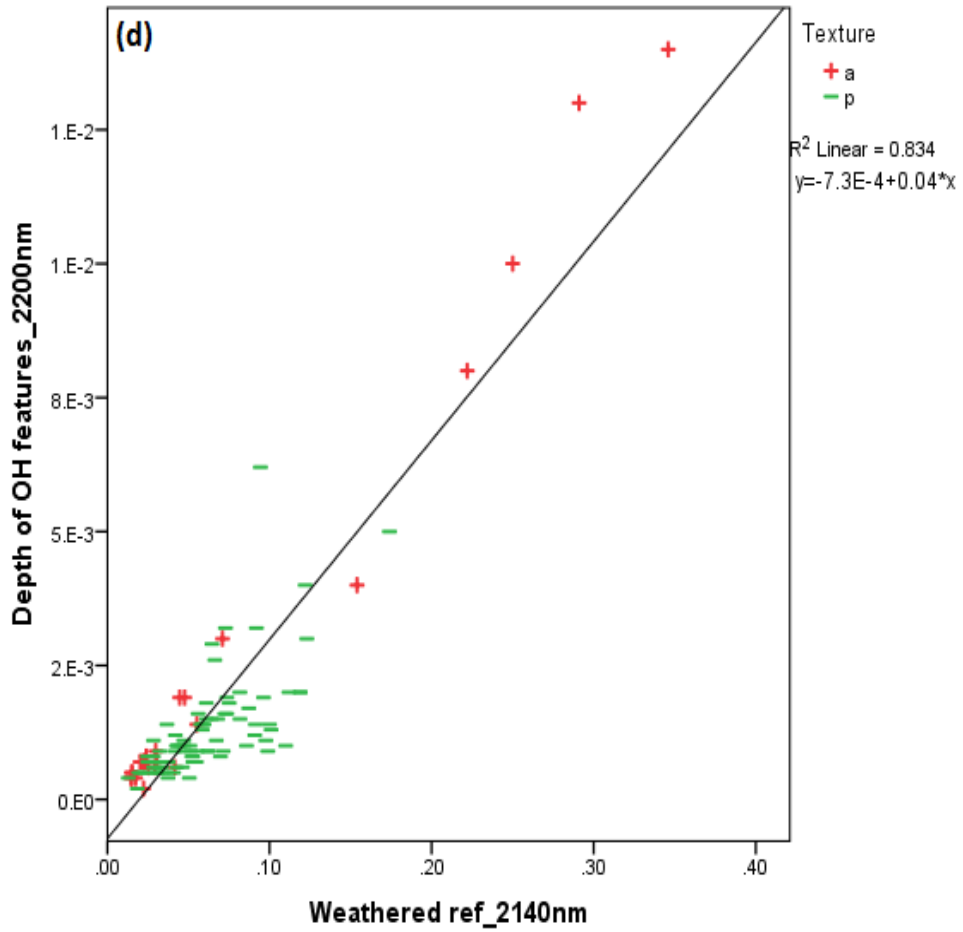


Figure 15: Scatter plots of the reflectance of rock samples against the different indices (a) (1900nmD) vs. reflectance at 1850 nm, weathered; (b) (1900nmD) vs. reflectance at 1850nm; (c) (1900nmD) vs. reflectance at 1850nm unweathered; (d) (2200nmD) vs. reflectance at 2140 nm weathered; (e) (2200nmD) vs. reflectance at 2140 nm unweathered; p= porphyritic; a= aphanitic and D= depth. For figures a-e, data for 38 rock samples is plotted including all rock samples with historical ages, relative ages and absolute ages. The solid lines at different slopes represent the regression line.

The hydration is increasing with reflectance linearly as explained by its linear regression line. There is an indication that the porphyritic rock samples have generally higher depth as compared to aphanitic rock samples (Figure 15) which is also evident by their higher relative reflectance. In the unweathered surface of the rock samples the two depth parameters are not correlated with their respective reflectance spectra also are expressed by the low R² values (Figure 15 c&e).

The above result from the spectral indices complement the spectral curve data in ENVI plots that indicates the aphanitic samples have generally lower reflectance (darker) than the porphyritic samples which actually have higher reflectance (lighter).

We also wish to investigate the relationship between (1900nmD) vs. reflectance at 1850 nm in a second order polynomial function (Figure 15b). A clear relationship was observed although it is not in entire linear relationship. There is still some sort of relationship between reflectance and the depth at 2200nm (Figure 15d). Low reflectance at the shoulder gives low feature depth at 2200nm.

A plot of the average reflectance (reflectance at 1800nm) and the relative age of flows is shown in Figure 16. The plot shows some systematic increase of the reflectance (brightness) with age. Rock sample from 1775AD flow generally show higher reflectance (brightness) than rock sample from the 1900AD flow. The details (brightness, absorption depth and relative ages) of these selected rock samples and nomenclature of the corresponding raw file is found in Appendix 2.

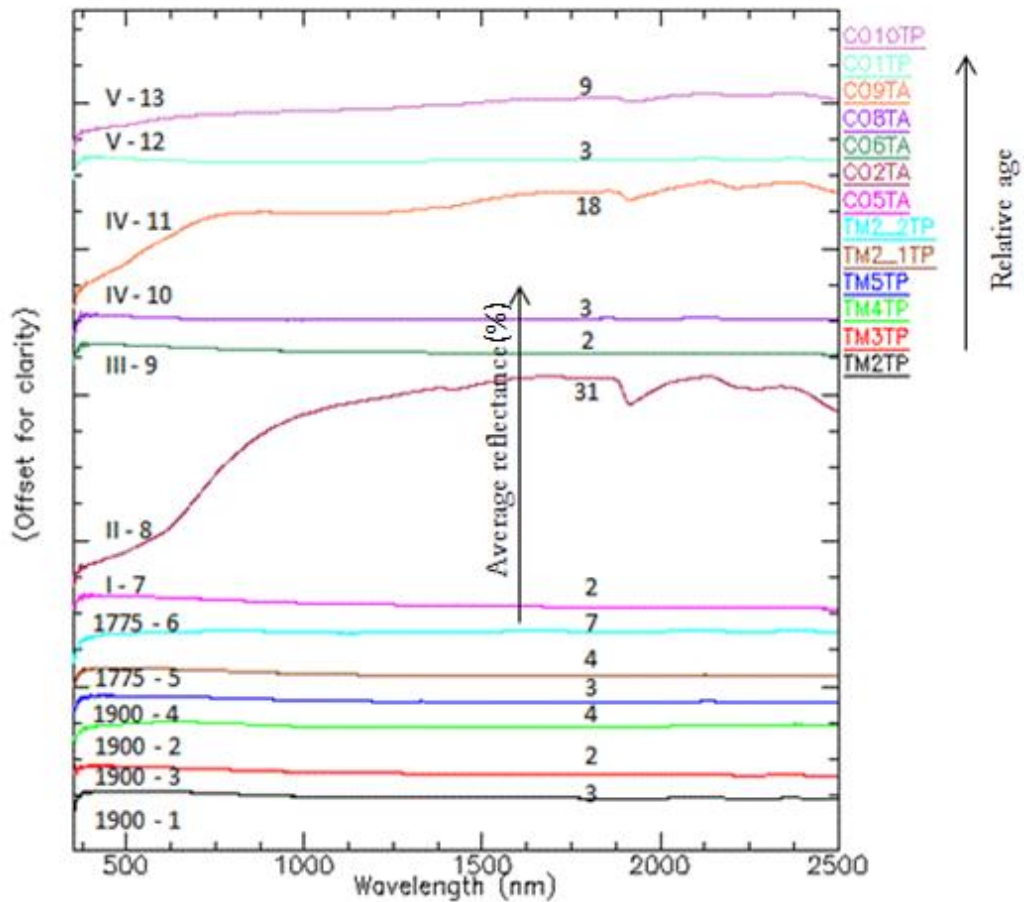


Figure 16: Laboratory average reflectance spectra of rock:- Laboratory average reflectance spectra of rock samples dating from 1900AD, (1900-1) rock sample TM2. (1900-2) rock sample TM3. (1900-3) rock sample TM4. (1900-4) rock sample TM5; 1775AD, (1775-5) rock sample TM2_1. (1775-6) rock sample TM2_2. (I-7) rock sample CO5. (II-8) rock sample CO2. (III-9) rock sample CO6. (IV-10) rock sample CO8. (IV-11) rock sample CO9. (V-12) rock sample CO1 and (V-13) rock sample CO10. Average reflectance values at 1800nm are indicated above each curve. Spectra have been offset vertically for clarity. Sample locations are indicated in Figure 4. 1900AD < 1775AD, I-7 < II-8 < III-9 < IV-10, IV11 < V-12, V-13 is the oldest.

For rough quantitative analysis, particular attention was given to the average brightness value observed at 1800nm for each rock samples. We studied the brightness versus age (absolute) for each OSL measured rock samples as well as rock samples from historical flows. These include rock samples from 7 flows: 115 years (TM1), 240 years (TM2), 199 years (CO5), 713 years (CO6), 208 years (CO8), 2064 years (AL9) and 11780 (AL17).

Based on the comments given on the OSL age results (e.g., number of aliquots, error estimates, comparability of the result with the relative geochronology data in-hand), only the data from sample CO5 and AL9 were included in the scatter plot in addition to the data from historical flows (TM1 and TM2). Figure 17 presents the relationship between the brightness and their absolute age.

The scatter plot shows that there is some sort of relation evident between brightness and age ($R^2=0.538$). Samples from early erupted flows (AL9) have a high brightness and vice versa but there are obvious weak side of the scatter plot. In the scatter plot, TM2 - from historic flow and CO5 are far from the trend.

Specifically the two samples from Tullu Moje historical flows (1900AD & 1775AD) showed brightness variation according to their ages. Brightness data is indicated in appendix2

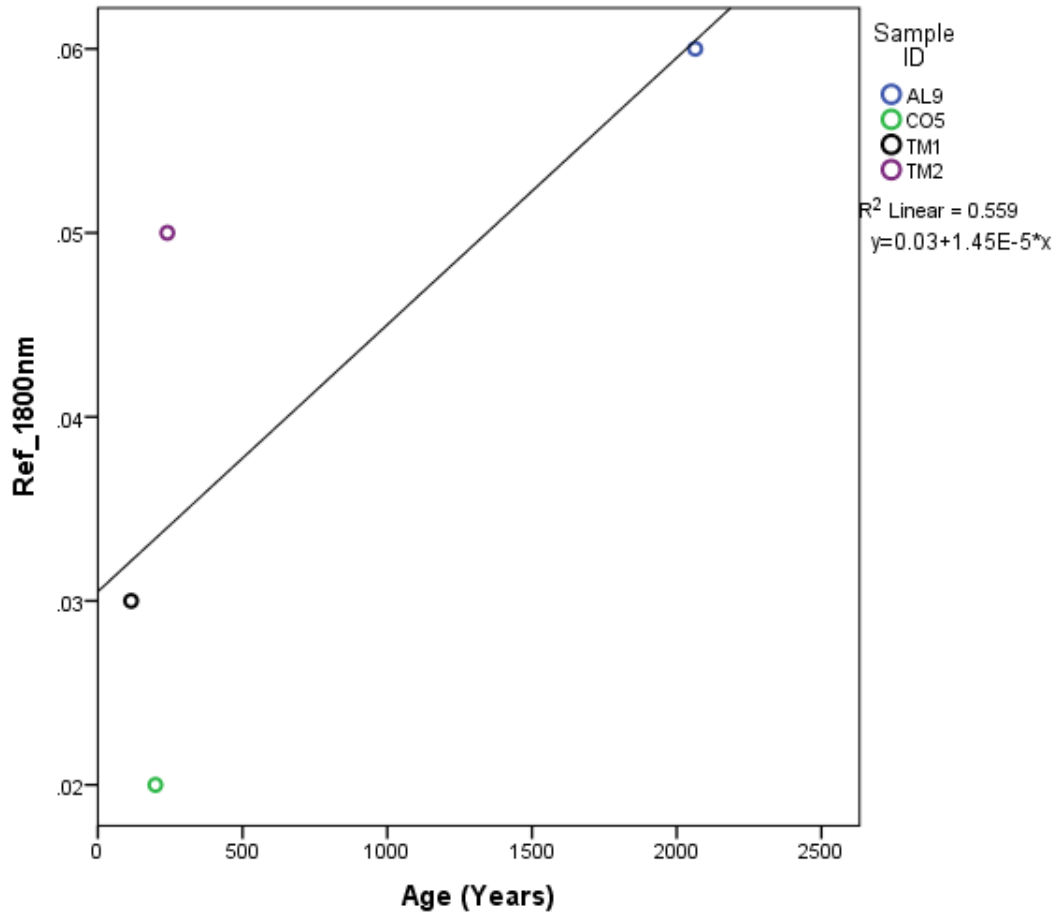


Figure 17: Scatter plot of the age of rock samples against their reflectance spectra (brightness). Reflectance values at 1800nm were used to represent the brightness of samples.

Inspired by the SWIR and the age relationship, a similar study for TIR was done. Based on 6 samples (TM2TP, CO5TA, CO6TA, CO8TA, CO1TP, CO10TP). The correlation of their per-channel emittance (6 values) with age (6 values) was calculated for all channels. The most significant correlation was found for the channel number 3844, wavelength 3.036 microns.

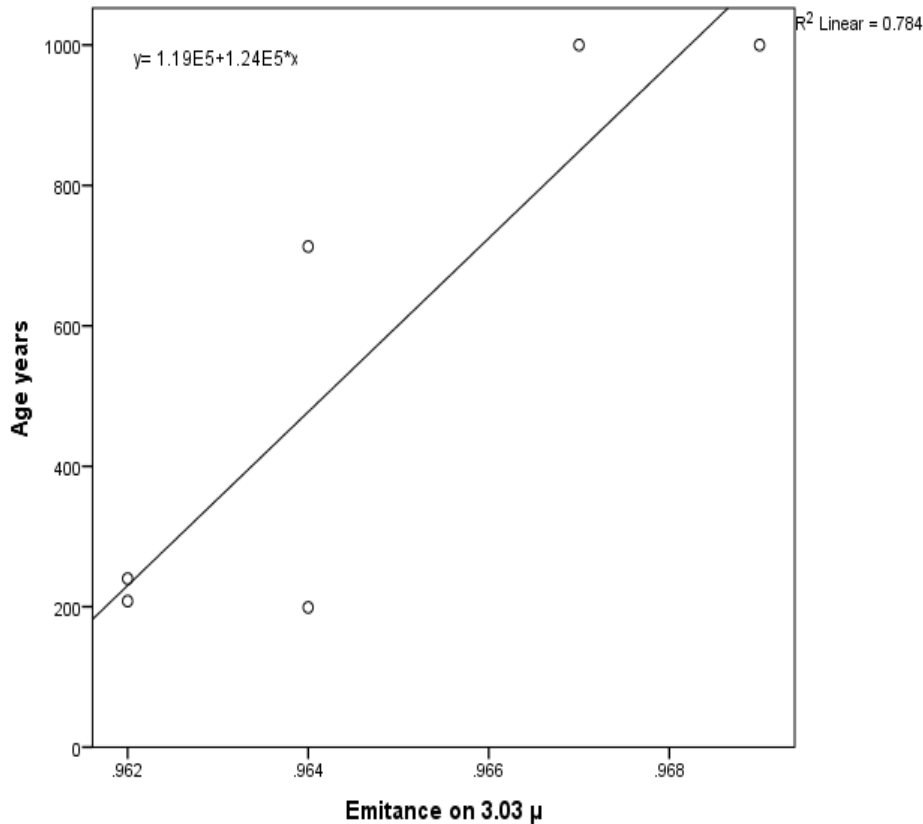


Figure 18: Scatter plot of the age of rock samples against their emittance at wavelength 3.036 microns

4.5. ASTER: Reflectance comparison (extrapolation)

The influence of other factors (e.g., vegetation density) on the reflectance spectra of the lava surfaces that might affect the relationship observed for rock samples in the lab was examined by plotting the reflectance versus NDVI values for selected region of interests. Such a graph is plotted in Figure 19, corresponding to the rocks sampling locations. It shows that ASTER 1650nm reflectance is not correlated with NDVI. ASTER 1650nm reflectance plotted for comparative purpose of the relative ages shows brightness increases as the lava age increases (Figure 20), for any two pixels, the pixel with the higher reflectance recognized higher relative age. The 1900AD flow is young-age hence have low reflectance than older flows.

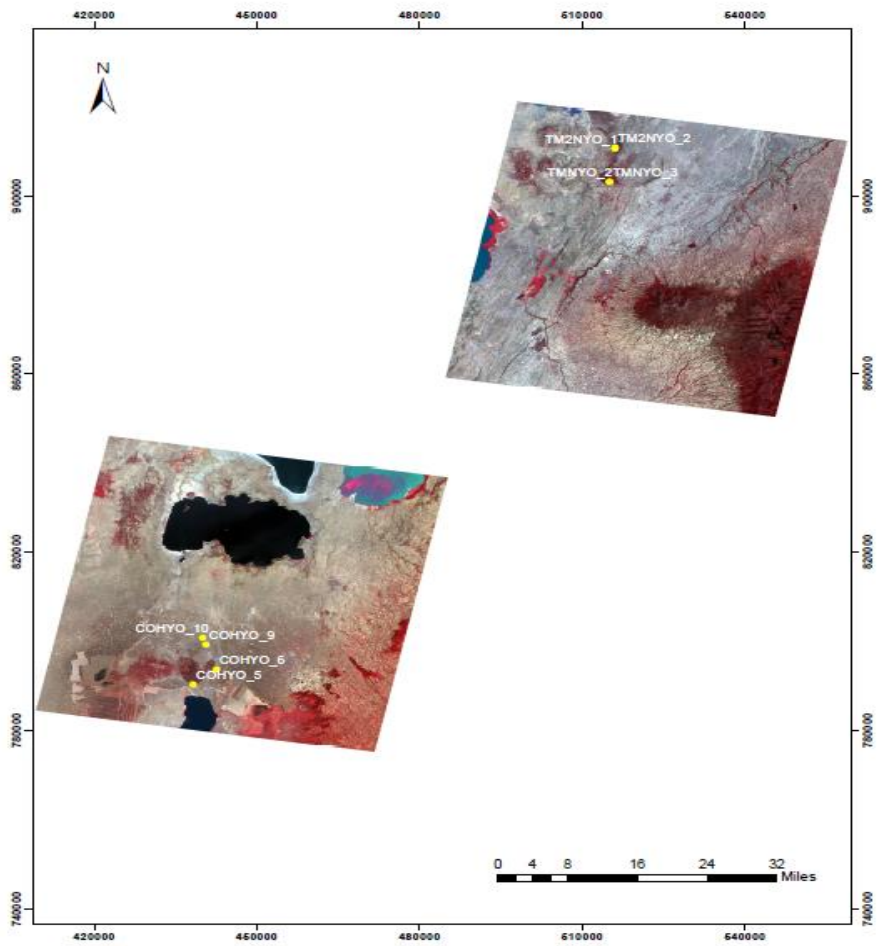


Figure 19: Location showing where the NDVI values extracted

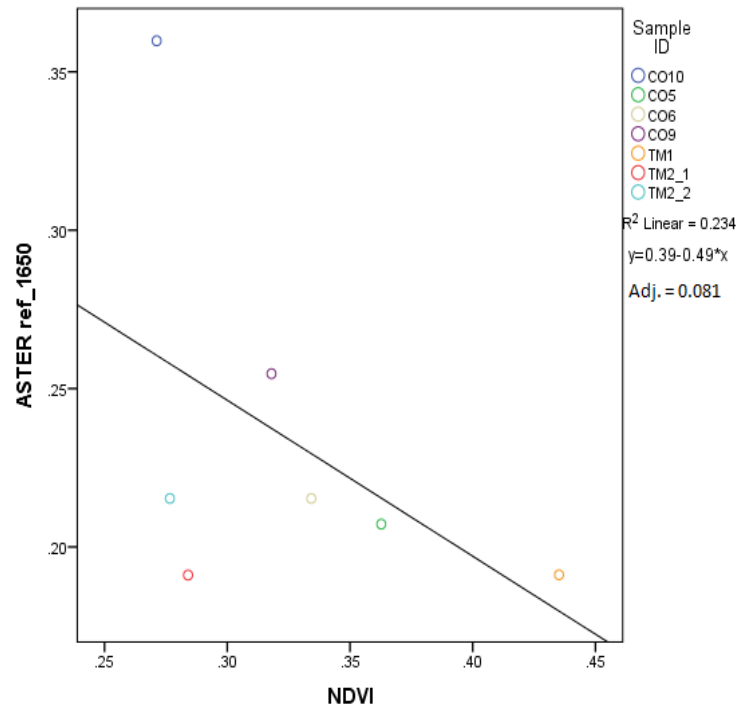


Figure 20 : Scatter plot of the reflectance at 1650nm in ASTER image of target regions against NDVI values.

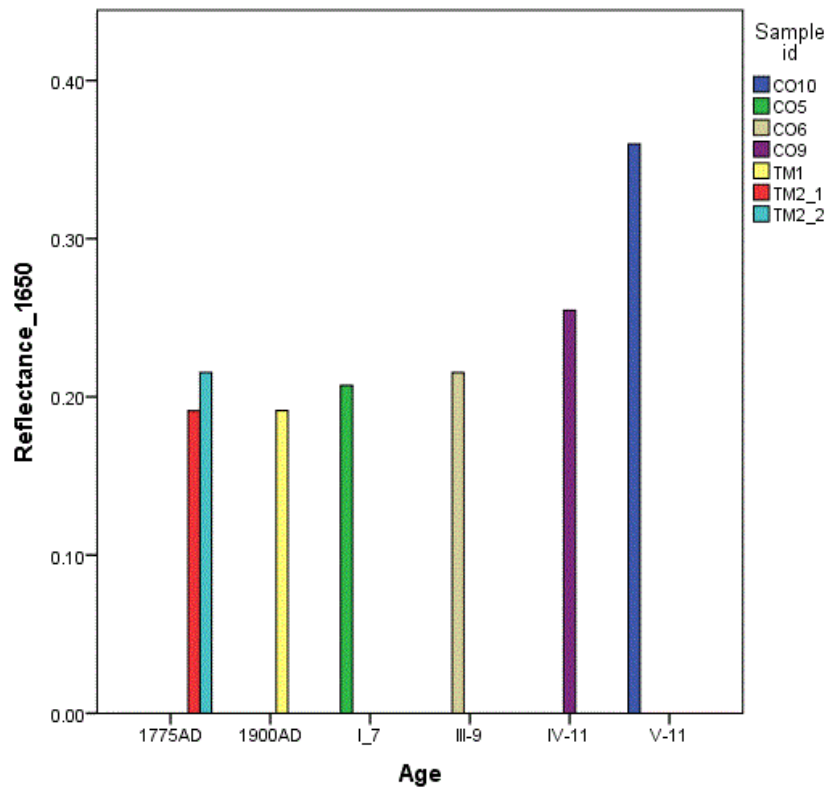


Figure 21: Reflectance at 1650nm of ASTER bands versus relative ages of lava flows.

5. DISCUSSION

5.1. Discussion

Many researchers have used the spectral behaviours of different volcanic environment to discriminate and map different volcanic products using satellite imagery (Kahle et al., 1988; Walsh, 1990; Abrams et al., 1991). The potential application of spectral data in relative dating of lava flows requires taking factors such as oxidation, vegetation, lichen cover into account. Although this application have been used for the past several years in the relative dating of lava flows, the current contribution, highlighting the contrasted spectral features of obsidians as a possible tool for absolute age determination is a first step towards other absolute dating technique that people might use it for dating and mapping of volcanic areas at least in limited areas.

5.2. Age-related variations in SWIR-TIR spectra of rock samples

The presence of reflectance spectra trend with age of the rock samples in the weathered than the unweathered (Figure 10a, b) suggests that the changes are most probably caused by weathering products attributed to hydration of the glass. The similarity in shape of the spectral curves for the weathered and unweathered surfaces of the same rock sample (e.g., Figure 11a) suggests the compositional similarity between the two surfaces. Spectral features are more pronounced on the weathered than unweathered surfaces which significantly affect the spectra. The thermal IR spectra of the samples can also discriminate between the two textures (Kahle et al., 1988).

In the SWIR spectra, the two absorption features (1900nm and 2200nm) show systematic trend with the reflectance spectra (Figure 10a). Below we discuss the link between the two spectral absorption features (1900nm and 2200nm) depth and their impact on the reflectance spectral of the rock samples of different ages.

The H₂O and hydroxyl spectral depth parameters, the depth about ~1900nm & ~2200nm, were associated with the weathering processes that results in formation or hydration of minerals that took place on the rock samples. These features are more pronounced and show systematics in the weathered than the unweathered surfaces with age (Figure 10a, b,c &d). This could most probably related to progression of the hydration and the physiochemical reaction on the top surface whilst the inside part might be thick and remains fresh not affected by external factors. The older rocks have higher depth of these features than the younger rocks (e.g., Figure 10, compare sample CO5TA & CO10TP), whilst in very young rock samples these features are almost disappearing. This indicates the progression of the hydration and/or weathering of the rock's surface since the time of emplacement. We are uncertain of the cause of sample CO2TA (second young in relative geochronology) to have a higher reflectance and hence higher absorption depth as compared to the older rock samples (Figure 10). The spectral curve for this specific sample resembles more to the curve of porphyritic samples. The main absorption feature for Illite is at the same wavelengths (near 1900nm & 2200nm) which probably indicate the presence of some clay mineral phases in the rock samples.

As discussed previously, the emissivity curve shape is indicative of the weathered and unweathered as well as the textural variations in the rock samples. Kahl 1988, attributed peak shape in thermal infrared reflectance spectra is more diagnostic than amplitude, which varies with sample particle size, surface roughness, and other characteristics. The major broad emissivity low of the spectra from 8 to 12 μ m centered near 9 μ m is in the general vicinity of the Si-O vibrational bands(Hook et al., 1994). This common emissivity low in the curve is most probably caused by some structured silica within the amorphous glass (e.g., Ericson et al., 1975; Ghasemzadeh et al., 2011). Possible explanations for the difference in emissivity low positions are spectral bands from the phenocrysts overlapping the glass band at wavelengths at ~ 9-10 microns and clay weathering products due to hydration.

The ordered behaviour of the reflectance with age in the rock samples is to some extent explained as a consequence of systematic changes to rock surfaces caused by hydration of the glass and/or weathering.

The following situations were observed. For aphanitic rocks, samples are associated with relatively low reflectance (spectrally dark) and have very weak spectral features, resulting subdued $\sim 1900\text{nm}$ & $\sim 2200\text{nm}$ depth. The aphanitic and porphyritic texture of the rock samples has essentially identical compositions; we attribute the subdued $\sim 1900\text{nm}$ of the aphanitic to weak hydration in the aphanitic than porphyritic texture. We attribute the two peaks longwards and the absorption between them ($\sim 2200\text{nm}$) is probably due to accumulation of some clay minerals.

Therefore reflectance for rock samples seems to be controlled by the texture (presence of the phenocrysts of most probably feldspar and quartz) and the degree of weathering that results formation or hydration of minerals. Unweathered and young rocks are associated with weak absorption depths; while the weathered and old rock samples have recognizable depth (Figure 10). It suggests that in the latter cases the surface of the rock may be more weathered, perhaps causing physiochemical alteration of the rock surface through hydration since the time of emplacement.

It seems that the two absorption features (H_2O and $-\text{OH}$) can be used for the relative reflectance variation (brightness) estimation by linking the features to hydration and/or weathering and level of crystallinity in the rock samples. For this to be true, it is necessary that texture also plays important role in the hydration process as water percolates more in porphyritic than the aphanitic texture, as texture controls rock surface porosity and will therefore influence rate of surface weathering (Medapati et al., 2013). This is in general true for the obsidian rocks we have studied.

We have noted the young age group in the TIR spectra contains both the porphyritic and aphanitic texture rock samples indicating the effect of texture in the TIR reflectance spectra is apparently low probably in very young rock samples but magnifies the spectral variation among rock samples is most attributed to ages accompanied by the hydration of the glass. This can be evident by figure 12b where both rock textures are contained in the same age group (young age group). However texture plays a role in the rest age groups (medium and old age groups) where rocks are grouped with respect to their texture.

5.3. Spectral indices and their relation to average brightness of rock samples

As previously noted, variation is observed within spectral curve shape of rock samples. The most prominent features in the SWIR, the water and hydroxyl features are evident, and are located at about 1900nm and 2200nm respectively.

The regression models obtained for these indices prove that depth of a water and OH feature depends on the brightness of the sample (Figure 15). The two indices (1900nm and 2200nm) have high adjusted R^2 values of 0.835 and 0.832 respectively. The results show that the 1900nm feature best characterizes the relationship between brightness of rock samples and their surface hydration and/or weathering. Weak relation trend in the unweathered surfaces (Figure 15c&e) suggest the similarity of the rock samples in original water content at the time of emplacement and the samples are still fresh and not affected by external factors.

5.4. Can XRD reveal mineralogical information in the weathered and unweathered surfaces in obsidians?

Based on the result from the XRD analyses of the four samples it could not be possible to quantify the mineralogy of the weathered and unweathered surfaces rather spectra of amorphous glass. This probably indicates the complexity to discriminate the different age groups of obsidian flows using any geochemical tool. This is also in agreement with the compositional similarities reported by (Rappich et al., 2013) among obsidian flows of the Corbetti volcanic system.

5.5. Is there any link between average brightness and relative ages in the Corbetti and Tullu Moje volcanic regions?

We have investigated whether the samples get brighter with age. We compared the reflectance at 1800nm for each average spectrum representing rock sample's brightness (albedo). The sample's spectrum show very flat spectra for the young rocks (Figure 11). Generally older rocks have higher reflectance at 1800nm and corresponding stronger absorptions near 1900nm and 2200nm . The absorption features seen at 1900nm are due to the presence of water. The absorption band near $2.2\mu\text{m}$ is pronounced in the oldest

rocks is probably due to the accumulation of a minor clay stage. We attribute the distinct absorption bands seen as shoulders near 1850nm and 2140nm to vibrational processes due to H₂O and OH such as the H–O–H bend with OH stretches in water bearing minerals and the combination of the metal OH bend and OH stretch in clay minerals (Clark, 1999).

A plot of the average reflectance for the spectrum shows some systematic increase of this value (brightness) with age. Also, the values of the H₂O feature depth increase with the observed brightness characteristics of the rock samples. The systematic progression of the brightness is therefore an indicator of the relative age of the rock samples, based on spectral reflectance variations most probably due to increasing hydration and/or weathering of the rock surfaces.

5.6. Is there a link between average brightness and absolute age dating?

Our results examine the use of reflectance property of obsidian to estimate age of flows under the same climatic conditions. The existence of a general brightness systematics at 1800nm implies that it may be possible to estimate flow age from obsidian reflectance spectra ($R=0.747$). The TIR spectra also suggest the emittance at 3.036 microns can be used to estimate the age in this partly qualitative way ($R=0.884$).

However, this method is far from complete. The reflectance systematics that we have seen reflects no support from petrographic geochemistry studies to quantify the mineralogy per unit area of the weathered and unweathered surfaces to link to the spectral data.

5.7. Interpretation of the ASTER observations

In Figure 19, we observed no correlation between the NDVI values with the reflectance at 1650nm. This indicates vegetation within the lava flows is not the dominant factor for the reflectance variation among the obsidian lava flows of the sample locations which are less or non-vegetated. Weathering, hydration of the glass, therefore, provides the best account for the reflectance variation among the lava surfaces at least for these non-vegetated lava targets. No exception is observed for all of the flows (flows from Tullu Moje and Corbetti volcanoes), which shows a higher reflectance than expected for its relative age (Figure 20). Based on the reflectance spectra at 1650nm against NDVI plot result, it appears that most of the variation in reflectance spectra of these obsidian flows is associated with weathering products of the lava surface most probably of hydration of the glass. Consequently, this reflectance variation facilitates the dating and mapping of lava flows simply taking non-vegetated areas, where we have obsidian flows erupted on top of previously erupted flows (older flows which are in the process of hydration) in the southern MER region.

6. CONCLUSIONS AND RECOMMENDATIONS

6.1. Conclusions

Our results examine the use of reflectance property of obsidian to estimate age of flows (relative or absolute) under the same climatic conditions. We proved that the more porphyritic a sample the more the 1900nm feature depth increases.

From our results, we conclude that:

- Aphanitic rock samples have low reflectance as compared to the porphyritic samples; porphyritic rock samples have generally higher absorption depth features as compared to aphanitic rock samples.
- Investigation of the spectral indices (water depth) indicates that beside its linear effect on the reflectance spectra, in terms of depth, the depth might go faster at a certain point than the

increase in reflectance. This is an important indication that the water absorption depth might not be in a 1:1 relationship with reflectance spectra for some of the rock samples studied.

- Weathering in the form of hydration can affect the spectra of rock surfaces considerably.
- Two distinct reflectance curves of the rock samples can be distinguished which differ in content of phenocrysts (feldspars) making them optically different from pure glass - this is very important result. Presence of phenocrysts modifies significantly the albedo and disables correlation with pure glasses.
- Very similar nature of the spectral curves that only differ by the presence of phenocrysts except for two outliers (CO2 and CO9), suggests that the satellite data can be compared directly (there is no other influence e.g., mineralogy).
- Some qualitative systematics is evident for rock samples on weathered surfaces based on the relative geochronology from Corbetii volcanic region and historical ages from TulluMoje volcanic region. Brightness of the rocks increase as rocks age.
- Extrapolation of the laboratory spectra to ASTER data proves that vegetation is not the dominant factor for the reflectance variation of the obsidian flows at the sample locations. There is brightness difference in the ASTER images with relative flow age. This partially suggests the reflectance spectra variation from obsidian flows attributed to weathering that results in hydration of the glass facilitates the dating and mapping of lava flows simply taking non-vegetated areas of the lava surface.
- Surface texture has influence on the spectra of rock samples. Obsidians with phenocrysts differ in optical properties already at hand-sample scale, and their correlation with pure glasses must be done carefully.
(Abrams et al., 2015)

The existence of a general reflectance spectra systematics caused by weathering or hydration of the glass implies it can be possible to estimate flow ages from obsidian reflectance spectra. In partly qualitative way, the reflectance at 1800nm proves the possibility to estimate age of the lava flows. The Pearson correlation ($R=0.733$) and the p-value (0.0091) for the reflectance at 1800nm are significant, although qualitative. Pearson correlation ($R= 0.88$) for the emittance at 3.036 microns also suggests the possibility to estimate the age in this partly qualitative way. However, this technique is far from complete. The reflectance spectra changes that we have seen reflect no support from geochemical studies (e.g., petrography) to quantify the mineralogy per unit area of the weathered and unweathered surfaces to see if there is still a link to the spectral data. We selected the 1800nm (SWIR) as a reference point for the brightness of the spectrum. However similar ones may be found in other wavelength regions (e.g., in the VIS) that could be more linked to age. This study induces many applications in the future. Although the relation between the ages and the spectra is valid only in limited areas, such a relation, even in a limited area, that can help people to do mapping and avoid hazards.

6.2. Recommendation

Based on the results presented here above, there are some recommendations that would improve and complete this research:

- Effect of texture on reflectance spectra of obsidians should be thoroughly understood that will answer the concern to be taken during correlation of the spectra from the two textures.
- Difficulties to extract mineralogical information and interpretation of the XRD results for the weathered and unweathered surfaces were also due to the difficulties in sample preparation to cut a thin slice off the top surfaces. It would be helpful to do petrography analysis for the weathered and unweathered surfaces to identify minerals and structures of the rocks, total rock composition that gives an indication in what type of minerals could be formed by normative calculation. It is also important to make thin sections and describe the rocks under the microscope. The porphyritic rock samples could be interesting to determine the minerals, at least optically. These all information would help to know if there is still a link to the spectral data. Meantime the information on the geochemistry of the rock samples would help to clearly understand if original composition before eruption has any effect on the rock reflectance spectra.
- Computing for a new suggestive variable 'Sn' which may better correlate with the 'Age'. Sn to be derived one for each average spectrum, $n = 1, \dots, 38$. A multivariate analysis of the spectra with age would be helpful based on the promising result with scatter plots.

6.3. Limitations of the technique (reflectance spectra of obsidians as a tool for age determination)

- The heterogeneity of a single lava flow can reduce the certainty of the dating technique (e.g., obsidian lava can have bands with variable content of microvesicles). But with the advance in remote sensing techniques, this could be solved by analysing albedo of a representative polygon (which may be presumed to combine various facies), instead of single point (if possible).
- Extrapolation of laboratory spectra to remote sensing is not straight forward both spatially and spectrally. It is not simple and straight forward to extrapolate to results. One problem is scaling issue. There is probably a lot of works to be done just to scale from the laboratory to the image.

LIST OF REFERENCES

- (Abrams et al., 1991) Abebe Ayele, M. T. and S. K. (2002). *Abaya-Tulu Moyo_Gedemsa Geothermal* (Vol. 1). Abebe, T. (2000). Geological limitations of a geothermal system in a continental rift zone: example of the Ethiopian rift Valley. *Proceedings of the World Geothermal Congress 2000*, 2025–2030.
- Abrams, M., Abbott, E., & Kahle, A. (1991). Combined use of visible, reflected infrared, and thermal infrared images for mapping Hawaiian lava flows. *Journal of Geophysical Research*, 96(B1), 475. <http://doi.org/10.1029/90JB01392>
- Abrams, M., Bianchi, R., & Pieri, D. (1996). Revised Mapping of Lava Flows on Mount Etna , Sicily. *Photogrammetric Engineering and Remote Sensing*, 62(12), 1353–1359.
- Abrams, M., Tsu, H., Hulley, G., Iwao, K., Pieri, D., Cudahy, T., & Kargel, J. (2015). The Advanced Spaceborne Thermal Emission and Reflection Radiometer (ASTER) after fifteen years: Review of global products. *International Journal of Applied Earth Observation and Geoinformation*, 38, 292–301. <http://doi.org/10.1016/j.jag.2015.01.013>
- Amici, S., Piscini, A., & Neri, M. (2014). Reflectance Spectra Measurements of Mt . Etna : A Comparison with Multispectral / Hyperspectral Satellite. *Advances in Remote Sensing*, 3(December), 235–245. <http://doi.org/http://dx.doi.org/10.4236/ars.2014.34016>
- Anovitz, L. M., Cole, D. R., & Fayek, M. (2008). Mechanisms of rhyolitic glass hydration below the glass transition. *American Mineralogist*, 93(7), 1166–1178. <http://doi.org/10.2138/am.2008.2516>
- Bandfield, J. L. (2009). Effects of surface roughness and graybody emissivity on martian thermal infrared spectra. *Icarus*, 202(2), 414–428. <http://doi.org/10.1016/j.icarus.2009.03.031>
- Biggs, J., Bastow, I. D., Keir, D., & Lewi, E. (2011). Pulses of deformation reveal frequently recurring shallow magmatic activity beneath the Main Ethiopian Rift. *Geochemistry, Geophysics, Geosystems*, 12(9), 1–11. <http://doi.org/10.1029/2011GC003662>
- Buchner, J., Rapprich, V., Tietz, O. (2013). Cenozoic Magmatism in Central Europe 24. In *Revision of potentially hazardous volcanic areas in southern Ethiopia* (pp. 218–219). Gorlitz, Germany.
- Cheong, C. S. (2014). Optical dating of haydromagmatic volcanoes on the southwestern coast of jeju island, Korea.
- Chernet, T. (2011). Geology and hydrothermal resources in the northern Lake Abaya area (Ethiopia). *Journal of African Earth Sciences*, 61(2), 129–141. <http://doi.org/10.1016/j.jafrearsci.2011.05.006>
- Chorowicz, J. (2005). The East African rift system. *Journal of African Earth Sciences*, 43(1-3), 379–410. <http://doi.org/10.1016/j.jafrearsci.2005.07.019>
- Clark, R. N. (1999). *Spectroscopy of rocks and minerals, and principles of spectroscopy. Remote sensing for the earth sciences: Manual of remote sensing* (Vol. 3). <http://doi.org/10.1111/j.1945-5100.2004.tb00079.x>
- Crisp, J., Kahle, A., B., Abbott, E., A. (1990). Thermal Infrared Spectral Character of Hawaiian Basaltic Glasses. *Journal of Geophysical Research*, 95(B13), 21,657 – 21,669. <http://doi.org/DOI:10.1029/JB095iB13p21657>
- Di Paola, G. M. (1972). The Ethiopian Rift Valley (between 7?? 00??? and 8?? 40??? lat. north). *Bulletin Volcanologique*, 36(4), 517–560. <http://doi.org/10.1007/BF02599823>
- Ericson, J. E., Makishima, A., Mackenzie, J. D., & Berger, R. (1975). Chemical and physical properties of obsidian: a naturally occurring glass. *Journal of Non-Crystalline Solids*, 17(1), 129–142. [http://doi.org/10.1016/0022-3093\(75\)90120-9](http://doi.org/10.1016/0022-3093(75)90120-9)
- Ericson, J. E., Makishima, A., Mackenzie, J. D., & Berger, R. (1975). Department of Anthropology and Institute of Geophysics and Planetary Physics, University of California, Los Angeles, California, USA, 17, 129–142.
- Fattahi, M., & Stokes, S. (2003). Dating volcanic and related sediments by luminescence methods: a review. *Earth-Science Reviews*, 62(3-4), 229–264. [http://doi.org/10.1016/S0012-8252\(02\)00159-9](http://doi.org/10.1016/S0012-8252(02)00159-9)
- Feathers, J. K. (2000). An introduction to optical dating. *Geoarchaeology*. [http://doi.org/10.1002/\(SICI\)1520-6548\(200001\)15:1<81::AID-GEA5>3.3.CO;2-Y](http://doi.org/10.1002/(SICI)1520-6548(200001)15:1<81::AID-GEA5>3.3.CO;2-Y)
- Friedman, I., & Obradovich, J. (1981). Obsidian hydration dating of volcanic events. *Quaternary Research*, 16(1), 37–47. [http://doi.org/10.1016/0033-5894\(81\)90126-5](http://doi.org/10.1016/0033-5894(81)90126-5)
- Galbraith, R. F., Roberts, R. G., Laslett, G. M., Yoshida, H., Olley, J. M., Galbraith, R. F., ... Laslett, G. M. (1999). Optical dating of single and multiple grains of quartz from Jinmium rock shelter, Northern Australia: Part I, Experimental design and statistical models. *Archaeometry*, 41(2), 339–364. <http://doi.org/10.1111/j.1475-4754.1999.tb00987.x>

- George, W. O. (2008). The Relation of the Physical Properties of Natural Glasses to Their Chemical Composition. *The Journal of Geology*, 32(4), 353–372. Retrieved from papers://a0f45058-72ca-4dc9-be03-e459899c7713/Paper/p943
- Gianelli, G., & Teklemariam, M. (1993). Water-rock interaction processes in the Aluto-Langano geothermal field (Ethiopia). *Journal of Volcanology and Geothermal Research*, 56(4), 429–445. [http://doi.org/10.1016/0377-0273\(93\)90007-E](http://doi.org/10.1016/0377-0273(93)90007-E)
- Gimeno, D. (2003). Devitrification of natural rhyolitic obsidian glasses: Petrographic and microstructural study (SEM+EDS) of recent (Lipari island) and ancient (Sarrabus, SE Sardinia) samples. *Journal of Non-Crystalline Solids*, 323(1-3), 84–90. [http://doi.org/10.1016/S0022-3093\(03\)00294-1](http://doi.org/10.1016/S0022-3093(03)00294-1)
- Global Volcanism Program | Tullu Moje. (2013).
- Green, R. O., Eastwood, M. L., Sarture, C. M., Chrien, T. G., Aronsson, M., Chippendale, B. J., ... Williams, O. (1998a). Imaging spectroscopy and the Airborne Visible/Infrared Imaging Spectrometer (AVIRIS). *Remote Sensing of Environment*, 65(3), 227–248. [http://doi.org/10.1016/S0034-4257\(98\)00064-9](http://doi.org/10.1016/S0034-4257(98)00064-9)
- Green, R. O., Eastwood, M. L., Sarture, C. M., Chrien, T. G., Aronsson, M., Chippendale, B. J., ... Williams, O. (1998b). Imaging spectroscopy and the Airborne Visible/Infrared Imaging Spectrometer (AVIRIS). *Remote Sensing of Environment*, 65(3), 227–248. [http://doi.org/10.1016/S0034-4257\(98\)00064-9](http://doi.org/10.1016/S0034-4257(98)00064-9)
- Head, E. M., Maclean, A. L., & Carn, S. a. (2012). Mapping lava flows from Nyamuragira volcano (1967–2011) with satellite data and automated classification methods. *Geomatics, Natural Hazards and Risk*, 5705(January 2016), 1–26. <http://doi.org/10.1080/19475705.2012.680503>
- Hutchison, W., Mather, T. a., Pyle, D. M., Biggs, J., & Yirgu, G. (2015). Structural controls on fluid pathways in an active rift system: A case study of the Aluto volcanic complex. *Geosphere*, 11(3), 1–21. <http://doi.org/10.1130/GES01119.1>
- JICA. (2012). *The Study on Groundwater Resources Assessment in the Rift Valley Lakes Basin in the Federal Democratic Republic of Ethiopia*, Japan International Cooperation Agency (JICA), Kokusai Kogyo Co., Ltd., Ministry of Water and Energy (MoWE), The Federal Democrati.
- Kahle, A. B., Gillespie, A. R., Abbott, E. A., Abrams, M. J., Walker, R. E., Hoover, G., & Lockwood, J. P. (1988). Relative Dating of Hawaiian Lava Flows using Multispectral Thermal infrared images: A new Tool for Geologic Mapping of young Volcanic Terranes. *Geophysical Research*, 93(B12), 15239–15251. <http://doi.org/10.1029/JB093iB12p15239>
- Kawano, M., Tomita, K., & Kamino, Y. (1993). Formation of clay minerals during low temperature experimental alteration of obsidian. *Clays and Clay Minerals*, 41(4), 431–441. <http://doi.org/10.1346/CCMN.1993.0410404>
- Le Turdu, C., Tiercelin, J. J., Gibert, E., Travi, Y., Lezzar, K. E., Richert, J. P., ... Taieb, M. (1999). The Ziway-Shala lake basin system, Main Ethiopian Rift: Influence of volcanism, tectonics, and climatic forcing on basin formation and sedimentation. *Palaeogeography, Palaeoclimatology, Palaeoecology*, 150(3-4), 135–177. [http://doi.org/10.1016/S0031-0182\(98\)00220-X](http://doi.org/10.1016/S0031-0182(98)00220-X)
- Li, L., Canters, F., Solana, C., Ma, W., Chen, L., & Kervyn, M. (2015). Discriminating lava flows of different age within Nyamuragira's volcanic field using spectral mixture analysis. *International Journal of Applied Earth Observation and Geoinformation*, 40(AUGUST), 1–10. <http://doi.org/10.1016/j.jag.2015.03.015>
- Liritzis, I., & Laskaris, N. (2011). Fifty years of obsidian hydration dating in archaeology. *Journal of Non-Crystalline Solids*, 357(10), 2011–2023. <http://doi.org/10.1016/j.jnoncrysol.2011.02.048>
- Lofgren, G. (1971). Experimentally produced devitrification textures in natural rhyolitic glass. *Bulletin of the Geological Society of America*, 82(1), 111–124. [http://doi.org/10.1130/0016-7606\(1971\)82\[111:EPD'TIN\]2.0.CO;2](http://doi.org/10.1130/0016-7606(1971)82[111:EPD'TIN]2.0.CO;2)
- Lu, Z., & Dzurisin, D. (2014). *InSAR Imaging of Aleutian Volcanoes*. Berlin, Heidelberg: Springer Berlin Heidelberg. <http://doi.org/10.1007/978-3-642-00348-6>
- M. Ghasemzadeh, A. Nematy*, A. Nozad**, Z. H. and S. B. (2011). Crystallization Kinetics Of Glass-Ceramics By Differential Thermal Analysis, 55(2), 188–194.
- Mazzarini, F., Mazzarini, F., Pareschi, M., Pareschi, M., Favalli, M., Favalli, M., ... Boschi, E. (2006). Lava flow identification and ageing by means of LiDAR intensity: the Mt. Etna case. *Earth-Prints.Org*, 112. <http://doi.org/10.1029/2005JB004166>
- Medapati, R. S., Kreidl, O. P., MacLaughlin, M., Hudyma, N., & Harris, A. (2013). Quantifying surface roughness of weathered rock - examples from granite and limestone. *Geo-Congress 2013*, 12–128. <http://doi.org/10.1061/9780784412787.013>

- Mrázová, Š., & Gadas, P. (2011). Obsidian balls (marekanite) from Cerro Tijerina, central Nicaragua: Petrographic investigations. *Journal of Geosciences*, 56(1), 43–49. <http://doi.org/10.3190/jgeosci.086>
- Murray, A. S., & Wintle, A. G. (2000). Luminescence dating of quartz using an improved single-aliquot regenerative-dose protocol. *Radiation Measurements*, 32(1), 57–73. [http://doi.org/10.1016/S1350-4487\(99\)00253-X](http://doi.org/10.1016/S1350-4487(99)00253-X)
- Paola, G. M. D. (1976). Geology of the Corbetti Caldera Area (Main Ethiopian Rift Valley).
- Peccerillo, a., Barberio, M. R., Yirgu, G., Ayalew, D., Barbieri, M., & Wu, T. W. (2003). Relationships between Mafic and Peralkaline Silicic Magmatism in Continental Rift Settings: a Petrological, Geochemical and Isotopic Study of the Gedemsa Volcano, Central Ethiopian Rift. *Journal of Petrology*, 44(11), 2003–2032. <http://doi.org/10.1093/ptrology/egg068>
- Preusser, F., Degering, D., Fuchs, M., Hilgers, A., Kadereit, A., Klasen, N., ... Spencer, J. Q. G. (2008). Luminescence dating: basics, methods and applications. *Eiszeitalter Und Gegenwart Quaternary Science Journal*, 57, 1–2. <http://doi.org/http://dx.doi.org/10.3285/eg.57.1-2.5>
- Rapprich, V., Žáček, V., Verner, K., & Erban, V. (2015). Wendo Koshe Pumice: the Latest Holocene Silicic Explosive Eruption of the Corbetti Volcanic System (Southern Ethiopia).
- Rapprich, V., Žáček, V., Verner, K., Erban, V., Goslar, T., Bekele, Y., ... Hejtmánková, P. (2016). Wendo Koshe Pumice: The latest Holocene silicic explosive eruption product of the Corbetti Volcanic System (Southern Ethiopia). *Journal of Volcanology and Geothermal Research*, 310, 159–171. <http://doi.org/10.1016/j.jvolgeores.2015.12.008>
- Rapprich, v., Cizek, D., Daniel, K., Firdawok, L., Habtamu, B., Hroch, T., Kopackova, V., Malek, J., Malik, J., Misurec, j., Orgon, A Sebesta, J., Sima, Tsigehana, T., Verner, K., Yewubinesh, B. (2013). Hawasa subsheet Report. *Czech Geological survey/ Aquatest/ Geological Survey of Ethiopia, Prabh/ Addis Ababa, Czech Republic/ Ethiopia. Explanation Booklet to the Set of Geoscience Maps of Ethiopia at Scale 1:50,000, Subsheet 0738-C4 Hawasa, pp. 1-46, 1–46.*
- Rendell H. M., Steer, D. C., & Townsend, P. D., W. A. G. (1985). The emission spectra of TL from Obsidian. *Nucl. Tracks*, 10(4-6), 591–600.
- Sawakuchi, Andre o., giordano, Daniele, Mineli, Thays D., Nogueira, L., Abede, T. A. (2015). Moving away from quartz and feldspar: evaluation of OSL dating of other silicate minerals and volcanic glasses, 5508.
- Simon J. Hook, Karlstrom, Kenneth J.W. McCaffrey 4, 5 2 Calvin F Miller, 3 and Kwnnrh J.W. McCaffrey. (n.d.). Mapping the piute Mountains, California, with thermal infrared multispectral scanner (TIMS) images, 99(94), 15,605–15,622. <http://doi.org/10.1017/CBO9781107415324.004>
- Smoak, J. M. (2013). Encyclopedia of Scientific Dating Methods, (JANUARY), 1–5. <http://doi.org/10.1007/978-94-007-6326-5>
- Trua, T., Deniel, C., & Mazzuoli, R. (1999). Crustal control in the genesis of Plio-Quaternary bimodal magmatism of the Main Ethiopian Rift (MER): Geochemical and isotopic (Sr, Nd, Pb) evidence. *Chemical Geology*, 155, 201–231. [http://doi.org/10.1016/S0009-2541\(98\)00174-0](http://doi.org/10.1016/S0009-2541(98)00174-0)
- van der Meer, F. (2004). Analysis of spectral absorption features in hyperspectral imagery. *International Journal of Applied Earth Observation and Geoinformation*, 5(1), 55–68. <http://doi.org/10.1016/j.jag.2003.09.001>
- Walsh, D. (1990). Research Paper Relative Dating of Volcanic Flows on a Back-Arc Stratovolcano, (1990). Retrieved from <http://frontiersabroad.com/wp-content/uploads/2012/09/Daniel-Walsh.pdf>
- Wintle, A. G. (1973). Anomalous Fading of Thermo-luminescence in Mineral Samples. *Nature* 245, *Research Laboratory for Archaeology and the History of Art, University of Oxford*, 143–144. <http://doi.org/10.1038/245143a0>
- WoldeGabriel, G., Aronson, J. L., & Walter, R. C. (1990). Geochronology and rift basin development in the central sector of the Main Ethiopian Rift. *Geological Society of America Bulletin*, 102, 439–485. [http://doi.org/10.1130/0016-7606\(1990\)102<0439](http://doi.org/10.1130/0016-7606(1990)102<0439)
- Yamaguchi, Y., Kahle, A. B., Tsu, H., Kawakami, T., & Pniel, M. (1998). Overview of advanced spaceborne thermal emission and reflection radiometer (ASTER). *IEEE Transactions on Geoscience and Remote Sensing*, 36(4), 1062–1071. <http://doi.org/10.1109/36.700991>
- Žáček, V., Rapprich, V., Aman, Y., Berhanu, B., Čížek, D., Dereje, K., ... Verner, K. (2014). The Study on Groundwater Resources Assessment in the Rift Valley Lakes Basin in the Federal Democratic Republic of Ethiopia.

APPENDICES:

Appendix 1: Descriptions of rock samples collected and measured from the four volcanic regions

List of all measured rock samples. The following information is given based on column 2. Names of these samples consist of 3-4 characters: the first two letters are the abbreviation of the volcanic region where they were taken (TM—Tullu Moje; AL—Alutu; CO—Corbetti; KS—Korke Selewa; A— aphanitic; P— porphyritic; the first numbers show the number given to a specific flow, the second numbers show sample number given to the rock. In total, there are 38 rock samples collected and measured from different lava flows in September - November 2015. Last column shows which specific measurements were done on the rock samples. All rock samples are collected from obsidian lava flows; all rock samples are about 7cm*6cm.

Sample_ID	Sample_ID (in laboratory)	Coordinates(UTM)		Elevation (m)	appearance in sample	Color	Measure ment
	X	Y					
TMNYO_1	TM1_2	514985.2	903139.3	2230	with phenocrysts	Black	ASD
TMNYO_2	TM2	514975.3	903161.3	2238	with phenocrysts	Dark gray	ASD
TMNYO_3	TM3	514974.2	903161.4	2238	with phenocrysts	Black	ASD
TMNYO_4	TM4	514244.2	902733.4	2169	with phenocrysts	Black	ASD
TMNYO_5	TM5	516149.2	902504.4	2212	with phenocrysts	Black	ASD
TM2NYO_1	TM2_1	515958,2	910359,3	1829	with phenocrysts	Black	ASD+TIR
TM2NYO_2	TM2_2	515955.2	910766.4	1800	with phenocrysts	Black	ASD
TM3NYO_1	TM3_1	517406,2	912248,3	1761	with phenocrysts	Black	ASD
TM4NYO_1	TM4-1	518052.2	912307.4	1745	with phenocrysts	Dark gray	ASD+XRD
ALHYO_1	AL1	472422.2	864674.4	1895	with phenocrysts	Grayish black	ASD
ALHYO_2	AL2	472538.3	864810.4	1899	with phenocrysts	Grayish black	ASD
ALHYO_3	AL3	472537.3	864810.4	1899	with phenocrysts	Grayish black	ASD
ALHYO_4	AL4	472537.3	864810.4	1899	with phenocrysts	Black	ASD
ALHYO_6	AL6	473293.2	863194.4	1991	with	Grayish	ASD

					phenocrysts	black	
ALHYO_7	AL7	473524.3	863390.3	1998	with phenocrysts	Grayish black	ASD
ALHYO_8	AL8	474012.3	862652.4	1952	with phenocrysts	Grayish black	ASD+TIR
ALHYO_9	AL9	478936.3	859465.3	2047	with phenocrysts	Grayish black	ASD
ALHYO_10	AL10	479125.3	859553.4	2049	with phenocrysts	Black	ASD
ALHYO_11	AL11	479009.3	857295.4	1995	mainly glassy	Black	ASD+XRD
ALHYO_12	AL12	481247.3	859736.4	2143	with phenocrysts	Black	ASD+XRD
ALHYO_13	AL13	481012.3	860177.4	2129	with phenocrysts	Dark gray	ASD
ALHYO_14	AL14	479574.2	859235.3	-	with phenocrysts	Black	ASD
ALHYO_15	AL15	472131.2	863093.3	2050	with phenocrysts	Greenish black	ASD
ALHYO_16	AL16	471883.3	863304.4	1961	with phenocrysts	Black	ASD
ALHYO_17	AL17	476974.2	855452.4	1711	mainly glassy	Black	ASD+TIR
COHYO_1	CO1	438638.3	787819.4	1705	with phenocrysts	Grayish black	ASD+TIR
COHYO_2	CO2	437291.2	790258.4	1722	mainly glassy	Black	ASD+XRD
COHYO_3	CO3	437479.2	790386.4	1747	mainly glassy	Black	ASD
COHYO_4	CO4	435176.3	794534.3	1856	mainly glassy	Black	ASD+TIR
COHYO_5	CO5	438156.2	790387.4	1779	mainly glassy	Black	ASD+TIR +OSL
COHYO_6	CO6	442455.2	793830.4	1872	mainly glassy	Black	ASD+TIR +OSL
COHYO_7	CO7	442826.3	793615.4	1787	mainly glassy	Black	ASD ASD+TIR
COHYO_8	CO8	438709.2	799706.4	1809	mainly glassy	Black	+OSL
COHYO_9	CO9	440540.3	799306.4	1803	mainly glassy	Black	ASD
COHYO_10	CO10	439989.2	801006.3	1755	with phenocrysts	Grayish black	ASD+TIR
COHYO_11	CO11	431529.2	795997.4	2071	with phenocrysts	Grayish black	ASD+TIR
COHYO_12	CO12	433425.2	796303.4	1885	mainly glassy	Dark gray	ASD
KSDYO_1	KS1	377677.1	739605.4	1461	with phenocrysts	Greenish gray	ASD

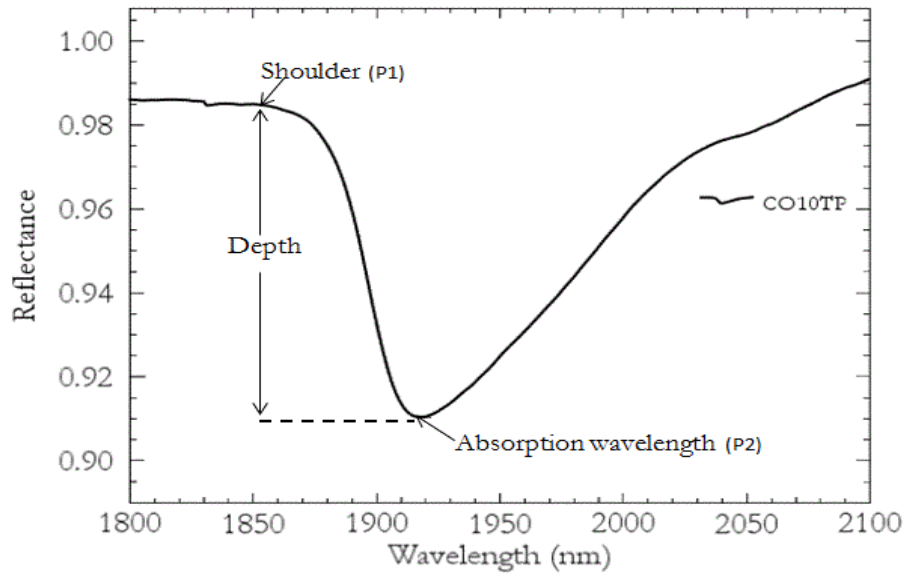
Appendix2: Rock samples selected for detail analysis of the spectra, nomenclature of the corresponding raw files, the two absorption depth values and the SWIR crystallinity values (X).

Sample (rock)	Age (relative)	Brightness (%)	Weathered		Unweathered	
			1900nmD	2200nmD	1900nmD	2200nmD
TMNYO_2	1900-1	3	0.01	0.12	0.01	0.1
TMNYO_3	1900-2	2	0.04	0.24	0.04	0.28
TMNYO_4	1900-3	4	0.06	0.3	0	0.3
TMNYO_5	1900-4	3	0.05	0.11	0	0.15
TM2NYO_1	1775-5	4	0.09	0.12	0.56	0.17
TM2NYO_2	1775-6	7	0.16	0.29	0	0.15
COHYO_5	I-7	3	0.06	0.11	0.03	0.06
COHYO_2	II-8	31	3.6	1.6	.03	0.09
COHNYO_6	III-9	2	0.04	0.08	.01	0.4
COHNYO_8	IV-10	3	0.11	0.12	.01	0.05
COHYO_9	IV-11	18	1.1	0.9	.07	0.26
COHYO_1	V-12	3	0.1	0.09	.03	0.17
COHYO_10	V-13	9	0.52	0.41	.28	0.31

Appendix 3: Example estimation of the water absorption feature.

In the spectrum, the absorption related with the water and OH features are recorded at 1900nm. The continuum - removal and feature extraction procedures were used to analyze individual spectra from laboratory ASD data. Two absorption points, P1 and P2, are taken to define the slop of the feature. P1 is the wavelength position of the 1850nm value, whereas P2 is the expected position of the minimum value for the water feature. D is the corresponding relative depth value of the water feature to calculate. The relative depth, D, of the absorption feature is defined as the reflectance value at the shoulders (in our case, at 1850nm) minus the reflectance value at the absorption band minimum.

Continuum removed - sample CO10 spectrum



Appendix4: Available eruption years. Tullu Moje volcanic region (historical and anthropology evidences); Corbetti volcanic region (14C) ages.

Volcanic region	Flow/Fall	Age	Evidence	Description
Tullu Moje	OR3	1900AD	Historical Observations	Obsidian
Tullu Moje	Tullu Moje	1775±25AD	Anthropology	Obsidian
Corbetti	WKpf	400BC	14C	WK Pumice

Note: BC= Before the death of Christ AD=After the death of Christ, WK= Wendo Koshe

OR3 = Youngest obsidian lava flows in Tullu Moje volcanic region

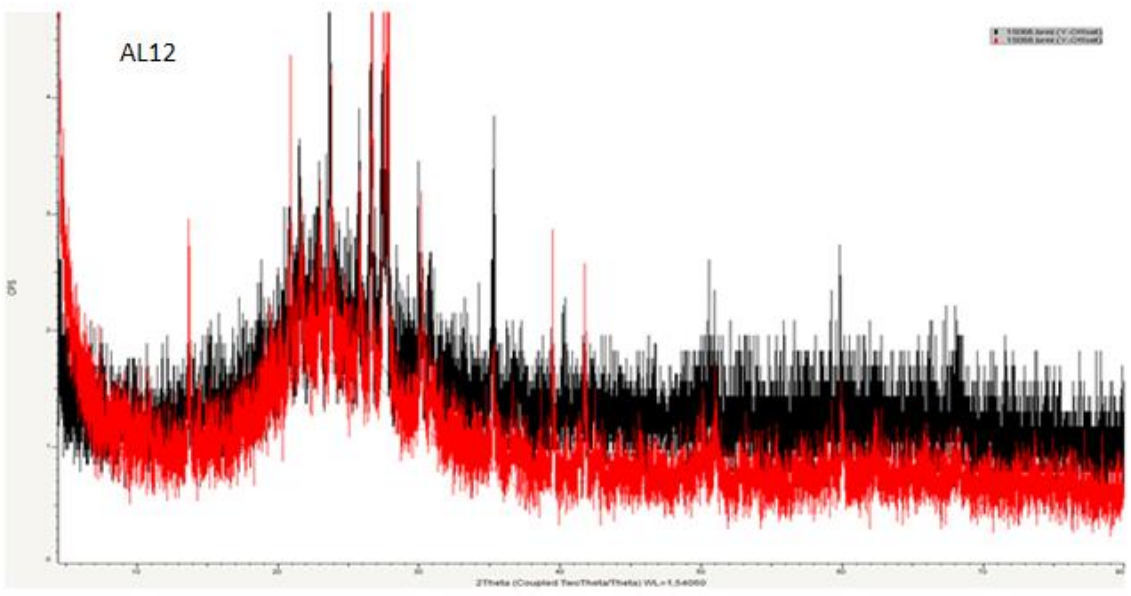
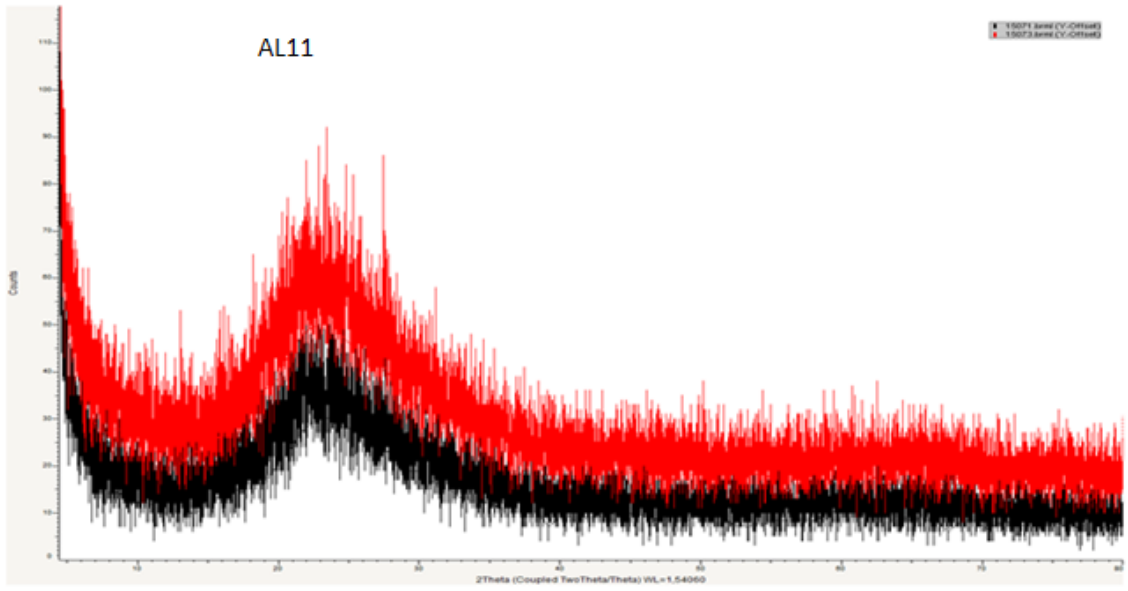
Tullu Moje = Oldest obsidian lava flow in Tullu Moje volcanic region

WKpf = Wendo Koshe pumice fall eruption (Young) in the the Corbetti volcanic region

Note: WKpf was post-dated by four obsidian lavas

Anthropology = anthropological study (analysis ranging from artifacts and evidence of past environments to architecture and landscapes)

Appendix 5: Results of XRD analysis: diffractograms. Samples show typical spectra of amorphous volcanic glasses. Aphanitic rock samples (AL11 and CO2); porphyritic rock sample (AL12); (black) Weathered surfaces; (red) unweathered surfaces.



Single-Aliquot Regeneration (SAR) dose protocol for equivalent dose estimation using Optically Stimulated Luminescence (OSL)

Luminescence measurements were carried out in a Risø TL/OSL DA-20 equipped with blue LEDs for stimulation, Hoya U-340 filters pack for light detection in the UV band and a built-in beta radiation source ($^{86}\text{Sr}/^{86}\text{Y}$) to give regeneration doses. The SAR protocol (described below) used for luminescence measurements was based on (Murray & Wintle, 2000), with an additional IR stimulation before blue stimulation to bleach eventual feldspar grains. Equivalent doses were calculated through the Central Age Model (Galbraith et al., 1999).

OSL-SAR protocol

1. Give Dose (D_i)
2. Pre-heat at 200°C for 10s
3. Infrared stimulation at 125°C for 100s
4. Blue light stimulation at 125°C for 40s (L_x)
5. Give test dose (D_t)
6. Pre-heat at 160°C for 0s
7. Infrared stimulation at 125°C for 100s
8. Blue light stimulation at 125°C for 40s (T_x)
9. Blue stimulation at 280°C for 40s
10. Return to step 1

Given doses D_i : $D_1 < D_2 < D_3 < D_4$; $D_5 = 0 \text{ Gy}$; $D_6 = D_1$

L_x/T_x : corrected OSL signal

Recuperation calculated through the ratio between the corrected signals of D_5 and D_n (natural dose)

Recycling ratio calculated through the ratio between the corrected signals of D_6 and D_1

The infrared stimulation was used to bleach feldspar signals. We used a quartz-like signal for equivalent dose estimation (post-IR blue).

Dose recovery test

The dose recovery test evaluated the capacity of the polymineral aliquots as radiation dosimeters using the OSL-SAR protocol (sequence described above). The dose recovery test was performed with 10 aliquots of sample COHYO-5. We used a preheat temperature of 200°C and a given dose of 40Gy. The calculated-to-given dose ratio was 1.04 ± 0.08 for 5 aliquots. Five among 10 aliquots were rejected due to inadequate recycling ratio and/or recuperation. Despite the rejection of 50% of the measured aliquots, the calculated-to-given ratio of 1.04 indicates that the polymineral aliquots can be used as reliable radiation dosimeters using the proposed OSL-SAR protocol.”

Appendix7: Results of the OSL dating of rock samples and comments on the result

“The dose recovery test was performed with 10 aliquots of sample CO-5. We used a preheat temperature of 200°C and a given dose of 40Gy. The calculated-to-given dose ratio was 1.04 ± 0.08 for 5 aliquots. Five among 10 aliquots were rejected due to inadequate recycling ratio and/or recuperation. Despite the rejection of 50% of the measured aliquots, the calculated-to-given ratio of 1.04 indicates that the polymineral aliquots can be used as reliable radiation dosimeters using the proposed OSL-SAR protocol.

Equivalent doses, dose rates and ages

Sample	Number of aliquots	Equivalent dose (Gy)	Overdispersion (%)	Average recycling ratio	Average recuperation (%)	Dose rate (Gy/ka)	Age (years)
AL-9	5	11.0±1.9	0	0.97±0.20	0	5.33±0.40*	2064±389
AL-17	2*	60.4±1.5	0	0.92±0.01	0.40±0.46	5.13±0.39	11780±943
CO-5	5	1.1±0.3	46	0.93±0.06	0	5.54±0.42	199±56
CO-6	4	3.8±1.4	62	0.98±0.16	0.57±0.41	5.33±0.40*	713±268
CO-8	1*	1.1±0.31	-	1.11	15.88	5.33±0.40*	208±16

Comments

Samples AL-17 and CO-8 have few aliquots (2 and 1) for equivalent dose calculation. Equivalent dose data are not statistically robust. Usually, we use at least 12 good aliquots per sample for equivalent dose calculation. Most of the measured aliquots were rejected, especially due to weak OSL signal.

Dose rate used for age calculation of AL-9, CO-6 and CO-8 samples is an average based on dose rates from samples AL-17 and CO-5. There was no time enough to prepare and measure those samples. We can measure further. However, the values should be not so different, considering very similar values obtained for the measured samples. "

Appendix 8: Rock samples and ages to study the TIR spectra

Sample Top	Estimated age	Oreder by age
TM2TP	240	3rd Young
CO5TA	199	1st young
CO6TA	713	2nd
CO8TA	208	young
CO1TP	Oldest	Oldest
CO10TP	Oldest	Oldest

Appendix9: Rock spectra locations and spectral files

The complete database that includes the volcanic regions, locations and spectral files of the laboratory data, sample names, rock description, and photographic record is attached in the digital version of this document.

